Wg Signaling via Zw3 and Mad Restricts Self-Renewal of Sensory Organ Precursor Cells in *Drosophila*

Janine C. Quijano, Michael J. Stinchfield, and Stuart J. Newfeld[1]
School of Life Sciences, Arizona State University, Tempe, Arizona 85287-4501

ABSTRACT It is well known that the Dpp signal transducer Mad is activated by phosphorylation at its carboxy-terminus. The role of phosphorylation on other regions of Mad is not as well understood. Here we report that the phosphorylation of Mad in the linker region by the Wg antagonist Zw3 (homolog of vertebrate Gsk3-β) regulates the development of sensory organs in the anterior–dorsal quadrant of the wing. Proneural expression of Mad-RNA interference (RNAi) or a Mad transgene with its Zw3/Gsk3-β phosphorylation sites mutated (MGM) generated wings with ectopic sensilla and chemosensory bristle duplications. Studies with pMad-Gsk (an antibody specific to Zw3/Gsk3-β-phosphorylated Mad) in larval wing disks revealed that this phosphorylation event is Wg dependent (via an unconventional mechanism), is restricted to anterior–dorsal sensory organ precursors (SOP) expressing Senseless (Sens), and is always co-expressed with the mitotic marker phospho-histone3. Quantitative analysis in both Mad-RNAi and MGM larval wing disks revealed a significant increase in the number of Sens SOP. We conclude that the phosphorylation of Mad by Zw3 functions to prevent the self-renewal of Sens SOP, perhaps facilitating their differentiation via asymmetric division. The conservation of Zw3/Gsk3-β phosphorylation sites in vertebrate homologs of Mad (Smads) suggests that this pathway, the first transforming growth factor β-independent role for any Smad protein, may be widely utilized for regulating mitosis during development.

INTERCELLULAR signaling is essential for proper development of multicellular organisms. In all animals, highly conserved proteins belonging to the transforming growth factor β (TGFβ) family perform a multitude of tasks. TGFβ proteins can be parsed into the TGFβ/Activin or Dpp/BMP subfamilies. In Drosophila, Dpp signals utilize the type I receptor Thickveins (Tkv), and signal transduction proceeds via Tkv phosphorylation of carboxy-terminal serines in the signal transducer Mothers against dpp (Mad). Once Receptor phosphorylated, Mad nuclear import occurs, and Mad then forms a complex with Medea. Mad/Medea complexes regulate gene expression together with tissue-specific transcription factors (Derynck and Miyazono 2008).

Mad and Medea are members of a highly conserved Smad family of TGFβ signal transducers. Mad and Smads1/5/8 in vertebrates signal for Dpp/BMP subfamily proteins while Medea and Smad4 in vertebrates form complexes with Smads that signal for all TGFβ proteins (Newfeld and Wisotzkey 2006). There are many instances during development when interactions between the TGFβ pathway and the equally ancient Wnt-signaling pathway are required. In brief, canonical Wg signal transduction begins with the Frizzled2 Receptor and proceeds via activation of Dishevelled (Dsh). Dsh then relays the signal to a ubiquitous cytoplasmic complex that includes Zw3 (Gsk3-β in vertebrates), dAPC, dAxin, and Armadillo (Arm; β-catenin in vertebrates). Under nonsignaling conditions, Zw3 phosphorylation continuously shunts the ubiquitously expressed Arm into the proteasome pathway for degradation. Upon receiving a Dsh signal, Zw3 is prevented from phosphorylating Arm. This leads to Arm nuclear accumulation and activation of gene expression in cooperation with transcription factors such as dTCF (Logan and Nusse 2004).

Frequently, the molecular mechanism underlying TGFβ–Wnt interactions is binding of Smad proteins to β-catenin and/or TCF. These complexes synergystically activate target genes via bipartite enhancer sequences (*e.g.*, Nishita *et al.* 2000). However, a phylogenetic analysis suggested the

doi: 10.1534/genetics.111.133801
Manuscript received July 14, 2011; accepted for publication August 13, 2011
Supporting information is available online at http://www.genetics.org/content/suppl/2011/08/25/genetics.111.133801.DC1.
[1]Corresponding author: Mail Code 4501, Arizona State University, Tempe, AZ 85287-4501. E-mail: newfeld@asu.edu

existence of another mechanism (Newfeld and Wisotzkey 2006). Conserved Zw3/Gsk3-β (serine–threonine kinase) sites were identified in all Mad/Smad1/5/8 subfamily members. Thus, it was predicted that Mad/Smad1 phosphorylation by Zw3/Gsk3-β represented a cytoplasmic mechanism of Smad–Wnt interaction. This prediction was subsequently confirmed. Fuentealba *et al.* (2007) demonstrated in vertebrates that Wnt stimulated Gsk3-β phosphorylation of Smad1, on serine in a central portion of the protein known as the "linker region", led to its degradation and the termination of TGFβ signaling.

Recently, an analysis in Drosophila employing a Mad transgene with its Zw3/Gsk3-β phosphorylation sites mutated (Mad-Gsk-sites-Mutant; UAS.MGM) and a phospho-specific antibody recognizing Zw3/Gsk3-β-phosphorylated Mad (pMad-Gsk) suggested that Mad is required for Wg signaling in wing development and segment patterning (Eivers *et al.* 2009). In contrast, Zeng *et al.* (2008) reported an analysis of Mad flip-out clones in wings in combination with biochemical studies. These authors concluded that Dpp signaling via Mad antagonizes Wg because Receptor-phosphorylated Mad outcompetes Arm for dTCF binding. Both studies utilized expression of the Wg targets Ac and Senseless (Sens) in sensory organ development as their assay.

Among the first steps in sensory organ development is the direct activation of Ac by Wg. In the wing disk, Ac is expressed in two rows of proneural cells arrayed along the proximal–distal (P/D) axis in the anterior compartment. These cells bracket the dorsal–ventral (D/V) boundary of the disk that expresses Wg, and they will become bristles on the wing margin. The dorsal row of Ac cells becomes a row of widely spaced chemosensory bristles on the dorsal surface while the ventral row becomes rows of stout mechanosensory bristles on the margin and interspersed thin mechanosensory and chemosensory bristles on the ventral surface (Blair 1992; Couso *et al.* 1994). Ac is also expressed in proneural cells that become the L1 and L3 sensilla on the anterior–dorsal surface.

Sens is also expressed in two rows of cells along the P/D axis of the wing disk (in a subset of Ac cells of the anterior compartment and extending into the posterior compartment) where it plays two roles in sensory organ development. Sens is a direct target of Wg on the ventral side of the anterior margin within a quadrant that is Apterous and Engrailed negative (Milan *et al.* 1998). Here Sens functions as a proneural gene in stout mechanosensory bristle formation and specifies sensory organ precursors (SOP) independently of Ac and Scute. On the dorsal side of the anterior margin, within a quadrant that is Apterous positive and Engrailed negative, Sens functions downstream of Ac and Scute in chemosensory bristle development. Here Sens specifies the SOP from within the group of Ac/Scute proneural cells. Along the posterior margin (Engrailed positive) Sens again acts as a proneural gene downstream of Wg and specifies a single row of non-innervated bristles on the margin (Jafer-Nejad *et al.* 2003, 2006).

The lineage that leads from a single Sens SOP to one type of adult sensory organ is well known: a mechanosensory notum bristle (Moore *et al.* 2004; Miller *et al.* 2009). In brief, notum bristle fate is initiated by Wg signals (Hayward *et al.* 2008). At stereotypic locations, Wg sets a prepattern by activating proneural genes such as Ac and Scute in groups of cells. This begins at 94–96 hr after egg laying (AEL) when Ac expression in the notum first becomes visible. One of the cells in this prepattern group activates Sens to become a SOP. This activates Delta–Notch-mediated lateral inhibition to prevent other prepattern cells from adopting a SOP fate. The SOP then undergoes three rounds of differentiation via asymmetric cell division (each division generates two distinct daughter cells, both of which are different from the parent). Each division is associated with the asymmetric inheritance of Numb, and the distinct identities of daughter cells are maintained by Notch signaling (Guo *et al.* 1996). The four terminally differentiated cells (shaft, sheath, socket, and neuron; a cell initially specified as glia undergoes apoptosis (Andrews *et al.* 2009) are visualized via differences in gene expression.

To address the paradox presented by Eivers *et al.* (2009) and Zeng *et al.* (2008) regarding potential roles for Mad in Wg signaling, we obtained the Zw3 phosphorylation-resistant Mad transgene (UAS.MGM) and the phospho-specific antibody (pMad-Gsk). We analyzed them utilizing Ac/Sens and sensory organ development in the wing. We found that Wg-dependent Zw3 phosphorylation of Mad limits self-renewing divisions in Sens expressing SOP. This restriction is spatially limited and occurs only during differentiation of sensory organs on the anterior–dorsal quadrant of the wing blade - chemosensory bristles and campaniform sensilla.

Materials and Methods

Drosophila stocks

Mutants are as described: *In(2L)dpp^{d5}*, *In(2L)dpp^{d6}*, *dpp^{hr4}*, *dpp$^{d\text{-}ho}$*, *In(2L)dpp^{s4} dpp$^{d\text{-}ho}$* and *In(2L)dpp^{s6} dpp$^{d\text{-}ho}$* (St. Johnston *et al.* 1990); *dSmad2^{MB388}* (Zheng *et al.* 2003); *gbb^{1}* and *gbb^{4}* (Khalsa *et al.* 1998); *Mad^{11}*, *Mad^{12}*, and *Df(2L)C28* (Raftery *et al.* 1995; Sekelsky *et al.* 1995); *Med^{7}* and *Med^{8}* (Wisotzkey *et al.* 1998); *sax^{1}* and *sax^{4}* (Twombly *et al.* 2009); *P{lacW}tkv^{k16713}* and *tkv^{7}* (Penton *et al.* 1994; Dworkin and Gibson 2006); and *zw3^{m11}* (Siegfried *et al.* 1992). Sca.Gal4 (Nakao and Campos-Ortega 1996) and MS1096.Gal4 (Milan *et al.* 1998) are as described. UAS strains are as described: CA-Tkv, CA-Sax, and DN-Tkv (Haerry *et al.* 1998); CA-Zw3 and DN-Zw3 (Bourouis 2002); CA-Notch (Fortini *et al.* 1993) and DN-Notch (Rebay *et al.* 1993); CA-Baboon (Brummel *et al.* 1999); dAxinΔRGS (Willert *et al.* 1999); Dpp (Staehling-Hampton and Hoffmann 1994); Dsh (Axelrod *et al.* 1996); Gbb (Khalsa *et al.* 1998); lacZ (Brand and Perrimon 1993); Mad (Newfeld *et al.* 1996); two independently generated lines of MadRNAi (Eivers *et al.* 2009 and Mike O'Connor, MN); and MGM

(Eivers *et al.* 2009) and Wg (Hays *et al.* 1997). Reporters are as described: Ac-LacZ (Van Doren *et al.* 1992), *P{en1}wg^{en11}* (Kassis *et al.* 1992), and *dpp*-lacZ-BS3.0 (Blackman *et al.* 1991). General stocks including lacZ and GFP balancers as well as FLP/FRT stocks for loss-of-function clones are described in FlyBase (Tweedie *et al.* 2009). Genetic analyses of wings and disks followed Takaesu *et al.* (2005) and Quijano *et al.* (2010).

Immunohistochemistry

Third instar larvae were staged utilizing 4-hr egg lays and aging for 116 hr before dissection, yielding a range from 116 to 120 hr AEL. Prepupae were staged by placing wandering third instar larvae into an empty vial, incubating them for 2 hr at 25°, and removing remaining wandering larvae but leaving white prepupae behind. Dissection of prepupae was performed 1 hr later, yielding a range in pupal ages of 1–3 hr after puparium formation (APF). During this stage wing disks evert into their adult orientation with only a modest increase in size (Aldaz *et al.* 2010); pupation proper begins 4–6 hr APF with the onset of cuticle secretion.

Larvae and prepupae were inverted and fixed in 4% formaldehyde/PEM, incubated in blocking solution [1% BSA/PBS with 0.1% Triton-X (PBST)], washed once with PBST, and incubated with primary antibodies at 4° overnight. Larvae were washed four times in PBST. Secondary antibodies were incubated overnight at 4°. Larvae then were washed four times in PBST and equilibrated in 70% glycerol/PBST. Wing disks were dissected, mounted in 70% glycerol/PBST, and sealed.

Hybridoma Bank antibodies were the following: mouse 22C10, mouse Achaete, mouse Cut (2B10), rat Elav (7E8A10), mouse lacZ (40-1A), mouse Pros (MR1A), mouse Repo (8D12), and mouse Wg (4D4). Additional primary antibodies were the following: mouse E(Spl)M8 (Jennings *et al.* 1994), mouse-cleaved Caspase-3 (Leinco), mouse pH3 (AbCam), rabbit lacZ (Organon Teknika), rabbit pMad-Gsk (Eivers *et al.* 2009), guinea pig pMad-SSVS (Persson *et al.* 1998; this is the well-known antibody against Receptor-phosphorylated Mad, which we distinguish from pMad-Gsk), guinea pig Sens (Nolo *et al.* 2000), rat Su(H) (Gho *et al.* 1996), guinea pig Sox15 and dPax2 (Miller *et al.* 2009), rat Hairy (Kosman *et al.* 1998), and rat Serrate (Papayannopoulos *et al.* 1998). Secondary antibodies were goat anti-mouse, rabbit, rat, and guinea pig Alexa Fluor 488, -546, and -633 (Molecular Probes) and biotinylated goat anti-rabbit (Vector Labs).

Images were taken capturing a 0.2-μm section every 2.0 μm. Intensity-averaged stacks were collected, and individual slices are shown for prepupal disks while stacks are shown for third instar larval disks. Larval and pupal wing disks were also analyzed with Vectastain Elite (Vector Labs), which detects biotinylated antibodies. Quantitative analysis of pMad-Gsk-, pH3-, and Sens-expressing cells employed image stacks for larval and prepupal disks. For pH3 and Sens studies in Sca.Gal4;Mad, Sca.Gal4;MadRNAi, and Sca.Gal4; MGM disks, we employed unpaired two-tailed *t*-tests to determine if the difference between two genotypes, in the average number of expressing cells, was statistically significant.

Results

Expression of UAS.MGM induces ectopic sensory organs independently of Dpp signaling

We first compared phenotypes generated by UAS.MGM to those of UAS.Mad and UAS.MadRNAi when expressed with an insertion in *scabrous* (Sca.Gal4). Sca is expressed during embryonic neurogenesis and again during larval and prepupal development. Sca is already visible in the epithelial precursors of proneural cells and their descendants in wing disks from the youngest third instar larvae (72–76 hr AEL; Powell *et al.* 2001). During late larval and prepupal wing development (Figure 1A, insets), Sca is expressed in a stripe adjacent to the anterior–posterior (A/P) compartment boundary on the anterior side (primordia of the L3 vein with three distal sensilla on its dorsal side) and two stripes bracketing the entire presumptive margin. The anterior margin primorida contain the precursors of the L1 vein and its two proximal sensilla on the dorsal side. The adult anterior margin contains three rows of bristles: widely spaced chemosensory bristles on the dorsal side, stout mechanosensory bristles atop the D/V boundary, and interspersed thin mechanosensory and chemosensory bristles on the ventral side. Atop the posterior margin there is a single row of non-innervated bristles.

Perhaps because Mad is normally ubiquitously expressed (Sekelsky *et al.* 1995), Sca.Gal4;UAS.Mad (Sca-Mad) generated wild-type wings 34% of the time (Figure 1A; Supporting Information, Table S1A) with the remainder displaying a variety of mild ectopic vein phenotypes. Alternatively, Sca.Gal4;UAS.MadRNAi (Sca-MadRNAi) always produced an abnormal phenotype, even in the presence of UAS.Mad. All Sca-MadRNAi wings were smaller than wild type and missing vein tissue. In addition, many displayed a second phenotype: ectopic sensilla on the Anterior Cross Vein (ACV), L1, and L3 veins and dorsal chemosensory bristle duplications (Figure 1B, Table S1B). The vein phenotype is consistent with prior studies of *Mad*. For example, studies of wing clones containing *Mad^{12}* (a deletion of the Receptor-phosphorylated serines; Sekelsky *et al.* 1995) or *Mad^{10}* (a missense mutation that abolishes Receptor phosphorylation; Hoodless *et al.* 1996) identified numerous defects in vein formation (*e.g.*, Marquez *et al.* 2001; Zeng *et al.* 2008).

In evaluating similarities and differences between the Sca-MadRNAi and *Mad* mutant clone phenotypes, it should be noted that Eivers *et al.* (2009) showed in Drosophila S2 cells that *Mad^{10}* and *Mad^{12}* produce full-length (or nearly so in the case of *Mad^{12}*) proteins amenable to phosphorylation by Zw3. Thus, at this time there are no genomic *Mad* alleles lacking the Zw3 phosphorylation sites; these were deleted in *Mad^{D14}* (Chen *et al.* 1998), but that allele has been lost. In

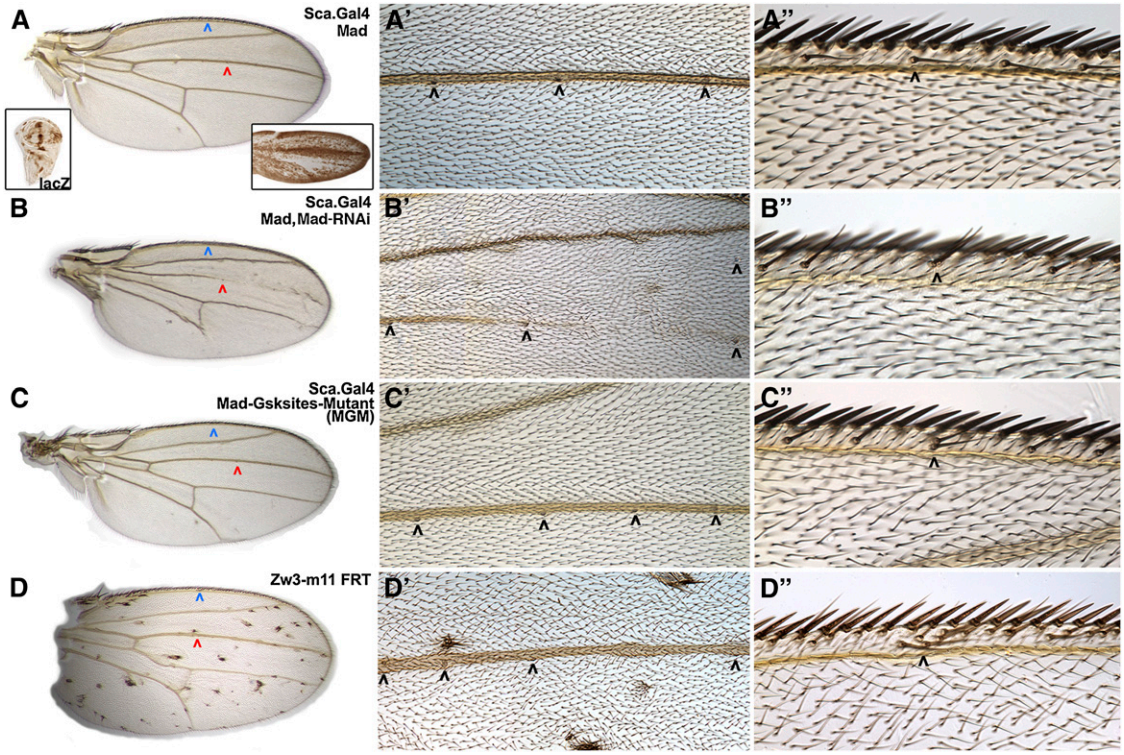

Figure 1 Ectopic sensory organs are generated by proneural expression of MGM. (A, A′, and A′′) Sca-Mad wing appears wild type with three sensilla on the dorsal side of vein L3 (red and black arrowheads) and a thin chemosensory bristle on the anterior–dorsal margin (blue and black arrowheads). Sca-lacZ is visible in the precursors of proneural cells and their descendants in larval (left inset) and pupal (right inset) wing disks (insets are not to scale with the primary image). (B, B′, and B′′) Sca-Mad,MadRNAi wing is missing portions of many veins including L3, but the L3 sensilla appear normal. An ectopic sensillum is present on the wing blade and a dorsal chemosensory bristle duplication (black arrowhead) is visible. Two independently generated MadRNAi lines produced the same phenotype. (C, C′, and C′′) Sca-MGM wing has no vein defects, but there are two ectopic sensilla on dorsal L3 (only four fit in the high-magnification view) and a dorsal chemosensory bristle duplication, a phenotype also seen with Sca-Mad, MGM. (D, D′, and D′′) Wing with numerous unmarked clones of the null allele $zw3^{M11}$ displays bunches of ectopic bristles on the wing blade and the margin. Ectopic sensilla are present on dorsal L3 (only four fit in the high-magnification view) and dorsal chemosensory bristle duplications are visible. See Table S1, A–D, for quantification of this phenotypic data.

addition, the smallest precisely defined deletion of *Mad* (*Df(2L)C28*; Wisotzkey *et al.* 2003) removes at least seven genes. These facts, taken together, suggest the possibility that the true null phenotype for *Mad* has not yet been identified. Thus the tissue-specific depletion of *Mad* transcripts with MadRNAi may be the best method available for approximating the *Mad* null phenotype and could reveal if *Mad* has non-Receptor phosphorylation-dependent functions.

Sca.Gal4;UAS.MGM (Sca-MGM) resulted in a mixture of wing phenotypes: wild type; ectopic veins; ectopic sensilla on the ACV, L1 and L3 veins; and dorsal chemosensory bristle duplications (Figure 1C, Table S1C). The fact that Sca-MGM ectopic vein phenotypes are more severe than Sca-Mad (*e.g.*, ectopic vein tissue extending from L2 is seen only with MGM) suggests that preventing Zw3 phosphorylation of Mad creates a gain-of-function allele capable of mimicking ectopic Dpp signaling. Thus one could conclude that Zw3 phosphorylation normally inhibits Mad's Receptor-dependent functions. This was noted by Eivers *et al.* (2009) on the basis of the ectopic expression of Dpp target genes in MGM wing disks.

Alternatively, the similarity of Sca-MGM and Sca-MadRNAi ectopic sensory organ phenotypes suggests that preventing Zw3 phosphorylation of Mad creates a loss-of-function allele for a previously unsuspected activity of Mad. In these experiments, MGM is expressed in otherwise wild-type wings and therefore must act as a dominant negative with regard to Zw3-dependent Mad functions. It seems likely that a Mad genomic null allele (eliminating Zw3 as well as Receptor phosphorylation) would generate a more robust sensory organ phenotype.

With the exception of sensilla to bristle transformation generated by Smad4 mutant alleles (Takaesu *et al.* 2005) and Eivers *et al.* (2009) studies of MGM, sensory organ phenotypes are not associated with Dpp in wing development. This led us to our first hypothesis: this newly uncovered activity of Mad in sensory organ development is independent of Dpp. Supernumerary sense organs (sensilla and bristles) are a hallmark of ectopic Wg signaling, as seen in wings with clones of the Wg antagonist *zw3* ($zw3^{M11}$; Figure 1D, Table S1D; *e.g.*, Blair 1992). The similarity of phenotypes generated by Sca-MGM (Zw3 phosphorylation-resistant Mad) and $zw3^{M11}$ clones (loss of *zw3* function)

suggests a second hypothesis: Zw3 phosphorylation of Mad is associated with Wg signaling. Furthermore, the disparity between the widespread presence of ectopic sensilla and all types of margin bristles in *zw3*^{M11} clone wings and the modest number of ectopic sensilla and dorsal chemosensory bristle duplications on the Sca-MGM wing suggests a third hypothesis: Zw3 phosphorylation of Mad is part of a spatially localized round of Wg signaling that influences only sensory organ development in the wing.

To evaluate the first hypothesis—Dpp independence of Zw3 phosphorylation of Mad—we conducted a comprehensive set of loss-of-function studies in wings employing mutant clones and viable hypomorphic genotypes for numerous Dpp pathway components. If the hypothesis is true, then it predicts that neither ectopic sensilla nor dorsal chemosensory bristle duplications will be present in any genotype. We analyzed *dpp*, *Mad*, *Medea*, *tkv*, *gbb*, and *sax* mutants. Gbb is a Dpp/BMP subfamily member that signals through the type I Receptor Saxophone (Sax) and then Mad during wing-vein formation (Bangi and Wharton 2006). We also analyzed *dSmad2*^{MB388} clones. dSmad2 contributes to Activin signaling and was initially thought to regulate wing size but not patterning (Brummel *et al.* 1999). However, dSmad2 was recently proposed to antagonize Mad in wing veins on the basis of RNAi studies (Sander *et al.* 2010).

All 13 of these Dpp/Gbb pathway genotypes produced vein defects of varying severity, but none displayed ectopic sensilla or chemosensory bristle duplications (Figure S1, A–I; Table S2, A–M). In many of these genotypes, the ACV was missing or truncated due to reduced Dpp/Gbb signaling. However, in every instance the ACV sensillum, normally located atop the dorsal surface of the ACV, was present in its wild-type location or relocated slightly anterior to a position atop the dorsal surface of L3; *gbb*^{1}/*gbb*^{4} exemplifies the former (Figure S1G) while *dpp*^{s4}/*dpp*^{d6} exemplifies the latter (Figure S1A). In addition, like the ACV, the Sensilla of the Dorsal Radius appeared in its normal location on proximal L3 even when the L3 vein was completely missing (out of the field of view to the left in Figure S1, right column). These results are consist with Mullor *et al.* (1997) who reported that altering *dpp* expression does not impact the sensilla of the dorsal radius, the ACV, or L3. *dSmad2*^{MB388} clones did not generate any phenotypes.

To rule out the possibility that the sensory organ phenotype seen with Sca-MGM was associated with overactivation of Dpp or Gbb signaling specifically in Sca-expressing cells, we conducted additional experiments. First, employing Sca.Gal4 we analyzed UAS.Dpp, UAS.CA-Tkv, UAS.CA-Sax (Haerry *et al.* 1998), and UAS.CA-Baboon (Baboon is an Activin type I receptor upstream of dSmad2; Brummel *et al.* 1999) and UAS.Gbb. In this assay, Dpp and CA-Baboon resulted in absolute lethality, most likely due to Sca.Gal4 embryonic expression. CA-Tkv and CA-Sax (Table S2, N and O) generated ectopic veins but did not display ectopic sensilla or dorsal chemosensory bristle duplications. Gbb wings were largely wild type with a fraction displaying ectopic tissue between L1 and L2 (Table S2P) due to the role of Gbb in augmenting Dpp signaling at the wing periphery (Ray and Wharton 2001).

Second, we analyzed Mad, MadRNAi, and MGM with MS1096.Gal4 [expressed throughout the wing blade (Milan *et al.* 1998; Marquez *et al.* 2001)] to exclude an artifact due to the *P*-element insertion in *sca* that created Sca.Gal4. MS1096-Mad flattened the Dpp gradient that patterns all veins. The L3 vein that normally responds to maximum Dpp signaling was overgrown, but all other veins were reduced or absent. In contrast, the ACV sensillum and the L3 sensilla were present in their normal locations. These wings did not contain ectopic sensilla or dorsal chemosensory bristle duplications (Figure S1J, Table S1Q). MS1096-MadRNAi also flattened the Dpp gradient and generated wings with missing veins. Although L3 was truncated after 20% of its normal length ectopic sensilla were visible on dorsal L3 (Figure S1K, Table S1R). MS1096-MGM leads to ectopic veins with ectopic sensilla on dorsal L3 and dorsal chemosensory margin bristle duplications (Figure S1L, Table S1S). These results exclude the insertion in *sca* as the source of the Sca-MGM phenotype. Overall, the wing data support our first hypothesis that Zw3 phosphorylation of Mad is independent of Dpp signaling.

Zw3 phosphorylation of Mad in larval wing disks is dependent on Wg signal transducers

To test our second and third hypotheses—that Zw3 phosphorylation of Mad is dependent upon Wg and that Zw3-phosphorylated Mad functions in anterior–dorsal sensory organ development—we examined pMad-Gsk expression in third instar larval wing disks (116–120 hr AEL). We began by examining pMad-Gsk in disks expressing Sca-Mad, Sca-MadRNAi, and Sca-MGM genotypes, and we triple-labeled the disks with pMad-Gsk (green), Ac (red), and Sens (blue). Sens in the nucleus of SOP cells is shown in the blue channel due to its exceptional reliability.

Prior to our analysis we characterized Sca.Gal4 temporal and spatial expression to aid in interpreting the resulting phenotypes. Temporally, Sca.Gal4 expression is visible in early third instar larval wing disks while Ac expression on the presumptive wing margin is not visible until mid-third instar (Figure S2A and Van Doren *et al.* 1992). Spatially, Sca.Gal4 is expressed in many SOP that express Ac and/or Sens in both compartments (Figure S2, B and C). The D/V stripe of Sca expression that functions in L3 sensilla formation overlaps the anterior portion of the parallel stripe of *dpp* expression that lies just anterior to the A/P compartment boundary (Masucci *et al.* 1990). The P/D rows of Ac anterior margin expression end within the region of overlap between the Sca and *dpp* stripes. The Sca stripe coincides with the highest levels of Receptor-phosphorylated Mad in the anterior compartment (Figure S2, D and E).

We noted that both Ac and Sens are present in the L1 and L3 sensilla precursor region where Ac is widespread and includes Sens-expressing cells (Figure S2B). However, we

could find no reports describing the respective roles of Sens and Ac (proneural *vs.* SOP specification) in L1 and L3 sensilla formation. Their respective expression patterns suggest that the relationship between these genes in sensilla is the same as in chemosensory bristles. Thus, we conclude that Ac acts as a proneural gene and that Sens specifies the SOP for only two types of sensory organ in the anterior–dorsal quadrant of the wing.

In our initial experiments, Sca-Mad expression had no obvious effect on Ac or Sens (Figure 2A). In Sca-Mad disks, a subset of Ac and/or Sens cells along the margin and in the L1 and L3 sensilla regions co-expressed pMad-Gsk (Figure 2, B and C). Alternatively, pMad-Gsk expression was occasionally seen without Ac or Sens co-expression—perhaps explained by co-expression with other proneural proteins such as Asense or Scute (Cubas *et al.* 1991; Brand *et al.* 1993). In a subset of co-expressing cells, uniform (cytoplasmic and nuclear) pMad-Gsk is juxtaposed upon nuclear Ac and/or Sens (Figure 2B, inset). In other co-expressing cells, pMad-Gsk is strictly cytoplasmic (Figure 2C, inset). In larval disks, pMad-Gsk was present only in the anterior–dorsal compartment: along the margin pMad-Gsk was visible in the dorsal row of proneural cells with occasional expression in the posterior-most cells in the ventral row and in the L1 and L3 sensilla regions. pMad-Gsk expression was quite variable but visible in every disk.

In Sca-MadRNAi disks ($n = 17$; Figure 2D), even when co-expressing UAS.Mad, Ac and Sens expression were normal but pMad-Gsk was absent. In Sca-MGM disks ($n = 10$; Figure 2E), the same results were obtained. These studies demonstrate the requirement for Mad and its two Zw3 phosphorylation sites for pMad-Gsk expression. Since we were unable to detect endogenous pMad-Gsk expression without UAS.Mad overexpression (with the notable exception of Wg overexpression, described below), we always co-expressed UAS.Mad. Given this experimental regime, we employed the phenotypically wild-type Sca-Mad genotype (see Figure 1A) as our reference rather than wild type.

Next we examined pMad-Gsk in genotypes with modified Wg pathways. First, we analyzed Sca-CA-Zw3 [S9A affecting an inhibiting phospho-serine (Bourouis 2002); $n = 9$], a genotype with modestly reduced canonical Wg signaling. Second, we studied Sca-Dsh ($n = 19$), a genotype with significant overactivation of canonical Wg signaling. Notwithstanding their disparate effects on canonical Wg signaling, both genotypes lead to expanded pMad-Gsk within the anterior–dorsal quadrant (Figure 2, F and G). Each of these assays display the highest level of pMad-Gsk expression/function: in wild type, no expression is detected; in Sca-Mad genotypes, expression is detected but without phenotypic consequence; and in Dsh and CA-Zw3, elevated expression is detected with phenotypic consequences. Third, we analyzed Sca-DN-Zw3 [A81T affecting an invariant alanine in the kinase domain (Bourouis 2002); $n = 6$], a genotype with modest overactivation of canonical Wg signaling. Sca-DN-Zw3-expressing disks had no pMad-Gsk (Figure 2H). These results implicate the Wg pathway components Dsh and Zw3 in Mad phosphorylation.

Taken together, the Dsh, CA-Zw3, and DN-Zw3 results suggest an unconventional mode of Wg signal transduction: Dsh stimulation of Zw3 to phosphorylate Mad. This cascade contrasts with canonical Wg signaling in which Dsh prevents Zw3 phosphorylation of Arm (Figure S2F). To further explore this unconventional pathway, we examined pMad-Gsk in Sca-dAxinΔRGS disks [the deletion confers weak constitutive activity and modestly reduces canonical Wg signaling (Willert *et al.* 1999)]. Expression of Sca-dAxinΔRGS ($n = 9$; Figure 2I) had no substantive effect on pMad-Gsk. This result supports the suggestion that an unconventional Wg pathway stimulates Zw3 phosphorylation of Mad because in the canonical pathway Axin cooperates with Zw3 in the phosphorylation of Arm (Figure S2F).

To confirm our prior studies suggesting that sensory organ phenotypes in Sca-MadRNAi and Sca-MGM genotypes are unrelated to Dpp, we examined pMad-Gsk in Sca-DN-Tkv disks. DN-Tkv is an effective means of blocking Dpp signaling (Haerry *et al.* 1998), and Sca-DN-Tkv wings display crossvein defects (Figure S1I, Table S2J). We found that Sca-DN-Tkv had no substantive effect on pMad-Gsk expression ($n = 9$; Figure 2J).

Wings derived from disks with altered Wg-signaling (*e.g.*, Sca-CA-Zw3 or Sca-Dsh) displayed phenotypes consistent with the ectopic sensory organ phenotypes of Sca-MGM and are best explained by Wg activation of both its canonical pathway and the proposed unconventional Dsh-Zw3-Mad pathway. Sca-CA-Zw3 wings with significantly reduced Wg signaling but expanded pMad-Gsk display the opposite phenotype of Sca-MGM (no pMad-Gsk): Sca-CA-Zw3 wings have no L1 or L3 sensilla, are missing margin bristles of all types, and display occasional vein truncations (Figure 3A, Table S3A). We attribute the vein and sensilla defects in Sca-CA-Zw3 wings to an overabundance of Zw3-phosphorylated Mad and the margin defects to reduced canonical Wg signaling leading to loss of Ac. Sca-Dsh wings with significant ectopic Wg signaling and expanded pMad-Gsk also contain the opposite phenotype of Sca-MGM: no L1 or L3 sensilla and vein truncations that we attribute to an overabundance of Zw3-phosphorylated Mad (Figure 3B, Table S3B). We attribute the ectopic mechanosensory bristles on the dorsal margin in Sca-Dsh wings to ectopic canonical Wg signaling.

In addition to sensilla, vein, and margin defects similar to those of Sca-CA-Zw3, Sca-Dsh wings display distal L3 vein overgrowth with ectopic margin bristles on the overgrown region. This distal L3 vein phenotype is attributable to the loss of Notch signaling as Dsh also antagonizes the Notch pathway (Axelrod *et al.* 1996). For example, expression of a Mind bomb mutant transgene that also antagonizes Notch (Lai *et al.* 2005) (utilizing Dpp.Gal4 that overlaps the stripe of Sca.Gal4 expression underlying the L3 vein; see also Figure S2D) results in a phenotype with important similarities and differences in the Sca-Dsh L3 vein phenotype. The similarity is that both genotypes resulted in L3 vein distal

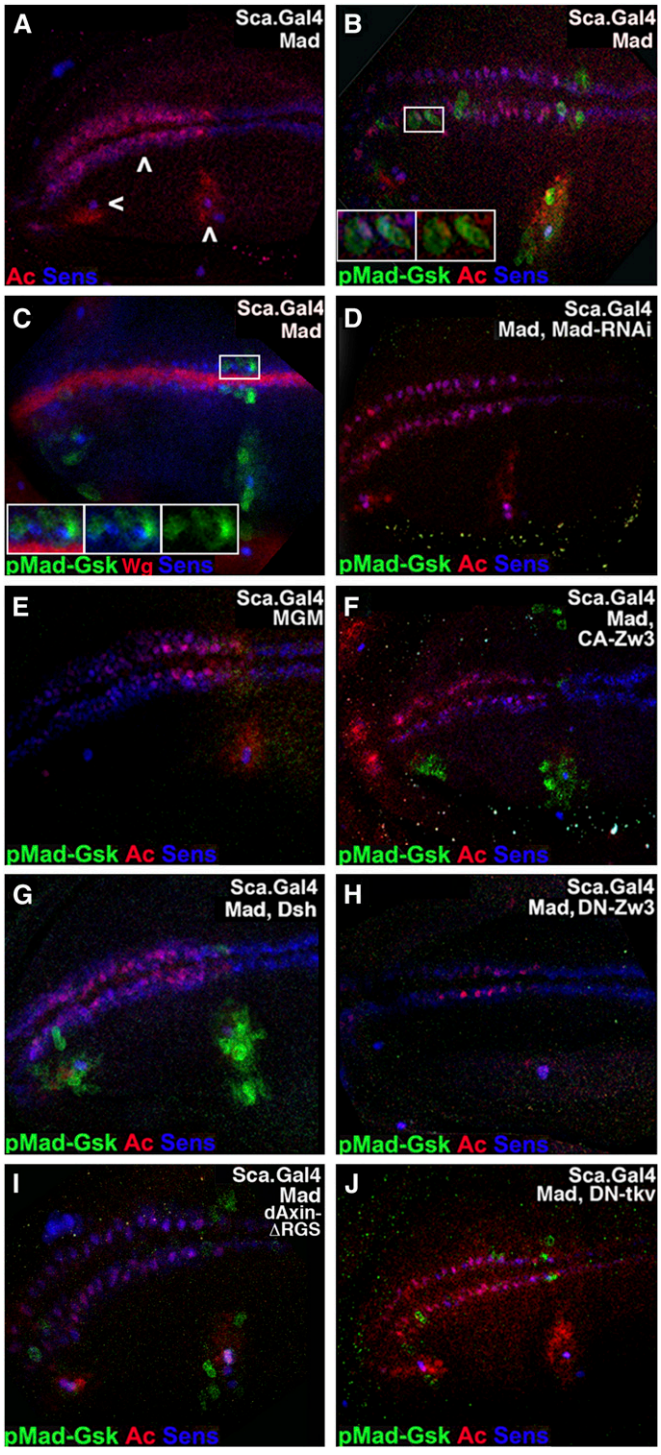

Figure 2 pMad-Gsk is expressed in larval wing SOP and responds to Wg signal transducers. Stacked confocal images of the presumptive wing blade from larvae aged 116–120 hr AEL with anterior to the left (as in Figure 1A, left inset) displaying pMad-Gsk (green), Ac (nuclear; red), and Sens (nuclear; blue) except as noted. We maintain this color scheme in Figures 2, 4, 5, 6, and 7. (A) Sca-Mad disk appears wild type with Ac and Sens in two rows of SOP (middle arrowhead; Ac anterior margin only). Ac and Sens expressing SOP for sensilla (L1: left arrowhead; L3: right arrowhead) are also visible. (B) Sca-Mad disk with several SOP on the dorsal margin and L1/L3 regions that express nuclear Ac and Sens and uniform (cytoplasmic and nuclear) pMad-Gsk. Boxed area is magnified twofold and shown as two insets to document the subcellular localization of pMad-Gsk: three-color (left) and two-color (pMad-Gsk and Ac; right). The ventral-most of the three pMad-Gsk cells to the right of the boxed area is a rare example that does not also express either Ac or Sens. (C) Sca-Mad disk labeled with Wg instead of Ac. Several cells on the margin and L1/L3 sensilla regions that express nuclear Sens also express cytoplasmic pMad-Gsk. Overall, pMad-Gsk was seen in 10.2 ± 6.7 cells ($n = 108$), 4.8 ± 4.5 anterior margin cells, 2.8 ± 2.8 L1 sensilla region cells, and 2.7 ± 2.1 L3 sensilla region cells. Insets: three-color (left), two-color [pMad-Gsk and Sens (middle)], and pMad-Gsk (right). (D) Sca-Mad,MadRNAi disk with no pMad-Gsk. (E) Sca-MGM disk with no pMad-Gsk, a phenotype also seen with Sca-Mad, MGM. (F) Sca-Mad,CA-Zw3 disk with expanded pMad-Gsk in the L1/L3 sensilla regions and ectopic pMad-Gsk on the ventral surface (above the margin rows). (G) Sca-Mad,Dsh disk displays expanded pMad-Gsk in the L1/L3 sensilla regions. (H) Sca-Mad,DN-Zw3 disk with no pMad-Gsk. (I) Sca-Mad,dAxinΔRGS disk similar to Sca-Mad (no effect on pMad-Gsk). (J) ScaMad,DN-Tkv disk similar to Sca-Mad (no effect on pMad-Gsk).

widening with multiple ectopic sensory organs (sensilla or bristles), which supports the notion that this aspect of the phenotype is due to loss of Notch. The difference is that the Mind bomb wing displayed multiple ectopic sensilla on the L3 vein while the Sca-Dsh wing lacked any sensilla on L3. This difference suggests that the absence of sensilla in the Sca-Dsh wing is not due to loss of Notch.

Sca-DN-Zw3 wings, with modest ectopic Wg signaling and no pMad-Gsk expression, weakly phenocopied wings with $zw3^{M11}$ clones, and the phenotype is again best explained by invoking the canonical and proposed unconventional (Dsh-Zw3-Mad) Wg pathways. Loss of the unconventional pathway explains why Sca-DN-Zw3 wings are similar to Sca-MGM wings with ectopic vein tissue and ectopic sensilla (Figure 3C, Table S3C). The presence of ectopic mechanosensory bristles on the margin is attributed to ectopic canonical Wg signaling. Wings with Sca-dAxinΔRGS that have modestly reduced Wg signaling [dAxinΔRGS is less potent than CA-Zw3 (Quijano *et al.* 2010)] and no impact on pMad-Gsk expression also did not contain defects in sensilla or chemosensory bristles (Figure 3D, Table S3D). We attribute occasional gaps in the stout mechanosensory bristle row to a reduction in canonical Wg signaling.

To better evaluate the hypothesis that expanded pMad-Gsk in Sca-Dsh wings is not associated with Notch, we conducted additional studies in larval wing disks. Cut is a transcription factor activated by Notch in an A/P stripe atop the wing margin (de Celis and Bray 1997) where it functions in D/V patterning. Cut is activated independently by proneural genes downstream of Wg in SOP where, like Sens, it persists and is required for sensory organ differentiation (Jarman and Ahmed 1998). pMad-Gsk is not visible in the Cut cells atop the margin but is visible in Cut and Sens SOP in the L1 and L3 sensilla regions (Figure 4A).

Hairy is a transcription factor downstream of Notch that is expressed in two intersecting stripes. One runs A/P along the margin while the other runs D/V atop the A/P compartment boundary and includes diffuse expression in the L3 sensilla region (Carroll and Whyte 1989, de Celis *et al.*

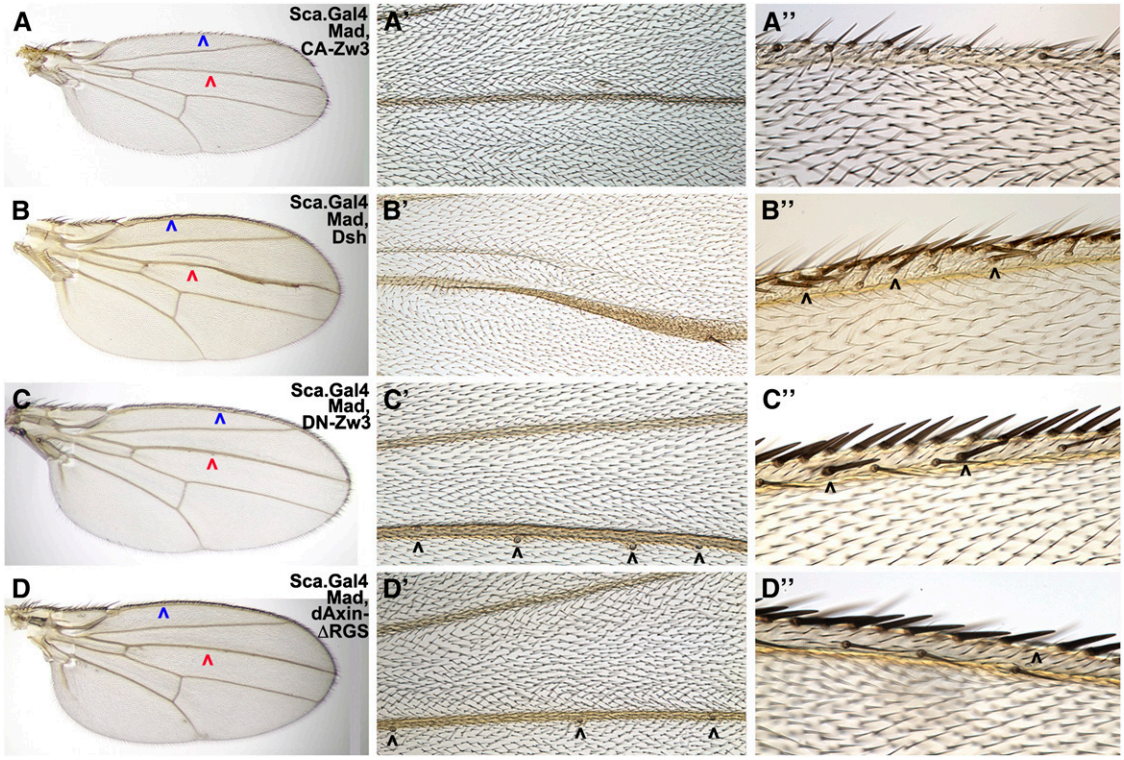

Figure 3 Ectopic sensory organ phenotypes of Wg signal transducers are similar to MGM. Wings derived from the same genotypes as shown in Figure 2. (A, A′, and A′′) Sca-Mad,CA-Zw3 wing with expanded pMad-Gsk has no sensilla on L3 (red arrowhead) and margin bristles of all types are missing (blue arrowhead). The presence of ectopic pMad-Gsk on the ventral side of larval wing disks, as shown in Figure 2F, does not appear to have any effect. (B, B′, and B′′) Sca-Mad,Dsh wing with expanded pMad-Gsk has no L3 sensilla and ectopic mechanosensory bristles on the dorsal margin (black arrowheads). The L3 vein is expanded distally and multiple margin bristles (all three types) are present in the overgrown region. (C, C′, and C′′) Sca-Mad, DN-Zw3 wing with no pMad-Gsk has two ectopic sensilla on a slightly thickened L3 [only four fit in the high-magnification view (black arrowheads)] and ectopic mechanosensory bristles on the dorsal margin. (D, D′, and D′′) Sca-Mad,dAxinΔRGS wing with normal pMad-Gsk has normal sensilla and occasional small gaps in the row of stout mechanosensory bristles.

1996). The A/P margin stripe is required for D/V patterning while the A/P compartment boundary stripe has no effect during larval stages but influences L3 sensilla location during pupal development (Blair *et al.* 1992). In larval disks, both pMad-Gsk and Sens are present within the diffuse Hairy domain in the L3 sensilla region (Figure 4B). Serrate (Ser) is a ligand for Notch expressed in stripes (like Ac and Sens) that bracket the D/V boundary and in the L1 and L3 sensilla regions. On the margin, the dorsal Ser stripe initiates Notch activity, leading to the activation of Cut in D/V patterning (Couso *et al.* 1995). Ser is not required for Notch-mediated lateral inhibition that identifies the SOP, and it functions redundantly with Delta during the asymmetric divisions of the SOP (Zeng *et al.* 1998). pMad-Gsk is expressed in several Ser and Sens cells on the margin and in the L1 and L3 sensilla regions (Figure 4C). These data suggest that Zw3 phosphorylation of Mad is independent of Notch as pMad-Gsk is present in cells without Notch signaling (Ser dorsal margin cells plus L1 and L3 SOP expressing Cut).

We then analyzed Mad, Wg, CA-Notch, and DN-Notch with wing-specific MS1096.Gal4 because Wg and Notch confer embryonic lethality with Sca.Gal4. Although these transgenes are also lethal with MS1096.Gal4, third instar disks can be examined (Quijano *et al.* 2010). As for Sca-Mad, we found that MS1096-Mad disks (Figure 4, D and E) displayed variable pMad-Gsk with no disks lacking expression. Ectopic pMad-Gsk is visible in non-Sens/non-Ac cells on the dorsal surface, but this has no effect on adult wings (Figure S1J). The disorganized margin expression of Wg, Ac, and Sens leads to mild irregularities in adult margin bristles.

MS1096-Wg disks contain a dense network of ectopic Ac and Sens cells in the anterior–dorsal quadrant, notwithstanding the fact that MS1096 is expressed throughout the wing blade (Figure 4F). As noted above, prior to this experiment, pMad-Gsk was detectable only in disks overexpressing Mad, but here Wg was capable of generating detectable levels of endogenous pMad-Gsk on the margin—consistent with our hypothesis that Wg stimulates an unconventional signaling pathway leading to Zw3 phosphorylation of Mad.

Alternatively, MS1096-DN-Notch disks displayed greatly reduced Ac and Sens at the margin but ectopic Ac and Sens in the L3 sensilla region. These disks did not display any pMad-Gsk on the margin (Figure 4G). MS1096-CA-Notch lethal disks generated ectopic Cut throughout the disk. This drastically reduced Sens, and these disks also did not

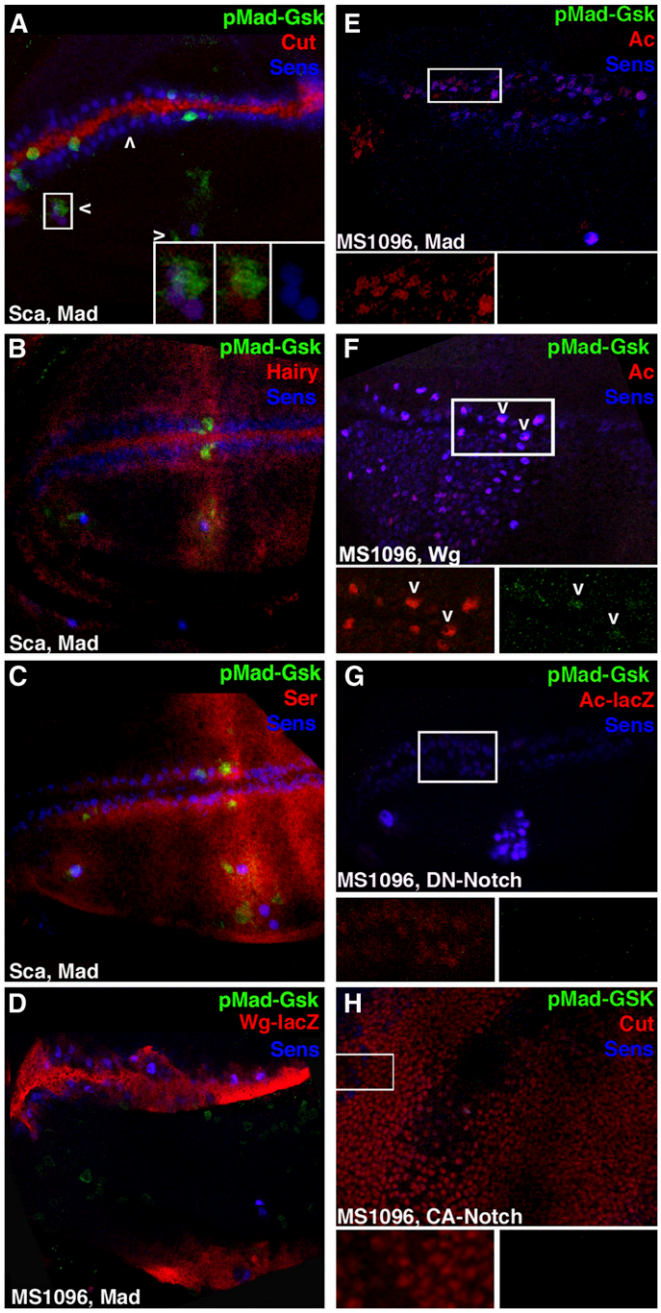

Figure 4 pMad-Gsk expression is dependent on Wg but not on Notch signaling. Stacked (A–C) and single confocal images (D–H) of the presumptive wing blade as shown in Figure 2 displaying pMad-Gsk (green), Sens (blue), and a cell-type-specific marker (red). Boxed areas are magnified twofold and shown in insets to better visualize pMad-Gsk expression. (A) Sca-Mad disk appears wild type with Notch-dependent Cut (nuclear; red) along the margin and Wg-dependent Cut in the L1/L3 sensilla regions. pMad-Gsk is expressed in multiple Cut and Sens cells in the L1 (left arrowhead) and L3 (right arrowhead) sensilla regions. (Insets) Three-color (left), two-color [pMad-Gsk and Cut (middle)], and Sens (right). (B) Sca-Mad disk appears wild type with Notch-dependent Hairy (nuclear; red) along the A/P boundary with diffuse expression in the L3 sensilla region and atop the D/V boundary but not in the L1 sensilla region. pMad-Gsk and Sens cells are visible within the diffuse Hairy domain in the L3 sensilla region. (C) Sca-Mad disk appears wild type with Ser (red) expression in two rows flanking the intersecting stripes of Hairy on the A/P and D/V boundaries plus diffuse expression in the L1 and L3 sensilla regions. pMad-Gsk is expressed in several Ser and Sens cells on the margin and in the L3 sensilla region. (D) MS1096-Mad disk with disorganized Wg-lacZ (red) and Sens on the margin. Sens generally brackets Wg-lacZ but is occasionally surrounded by Wg-lacZ cells. pMad-Gsk is present in two Sens cells in the dorsal bristle row and in numerous ectopic cells throughout the dorsal surface. Overall, pMad-Gsk was visible in 16.5 ± 14.9 cells ($n = 6$), 13.9 ± 12.6 anterior margin cells, 0.8 ± 1.3 L1 sensilla region cells, and 1.8 ± 1.5 L3 sensilla region cells. (E) MS1096-Mad disk with disorganized Ac (red) and Sens along the margin consistent with abnormal Wg-lacZ in this genotype. (Insets) Ac (red) on the left and pMad-Gsk (green) on the right. There is no pMad-Gsk expression on the margin but a single pMad-Gsk, Sens, and Cut cell is present in the L3 sensilla region (located under the right inset and not visible). (F) MS1096-Wg lethal disk with ectopic Ac (red) and Sens throughout the anterior–dorsal quadrant. (Insets) Ac (red) on the left and pMad-Gsk (green) on the right. pMad-Gsk is present in five cells along the margin (right) that co-express Ac and Sens. Two pMad-Gsk cells are indicated by arrowheads. (G) MS1096-DN-Notch lethal disk with greatly reduced Ac (red) and disorganized Sens at the margin but numerous ectopic Ac and Sens cells in the L3 sensilla region. (Insets) Ac (red) on the left and pMad-Gsk (green) on the right. No pMad-Gsk expression is visible. (H) MS1096-CA-Notch lethal disk with ectopic Cut (red) throughout the disk. Several Sens cells are present at random, and there is no pMad-Gsk. (Insets) Cut (red) on the left and pMad-Gsk (green) on the right. No pMad-Gsk expression is visible.

contain any pMad-Gsk (Figure 4H). Although the DN- and CA-Notch results do not formally exclude the possibility that Notch influences pMad-Gsk expression, the data clearly reveal that Wg plays a larger role on the basis of the visibility of pMad-Gsk without co-expression of Mad when Wg is overexpressed. Overall, we conclude that the pMad-Gsk larval disk studies and the corresponding Sca.Gal4 adult wing phenotypes support our hypothesis that Zw3 phosphorylation of Mad depends upon Wg.

Zw3-phosphorylated Mad is present in sensory organ lineage cells in prepupal wings

We then further tested our hypothesis that Zw3-phosphorylated Mad functions specifically in sensilla and dorsal chemosensory bristle development in the anterior–dorsal quadrant of the wing. Here we examined pMad-Gsk in Sca-Mad prepupal wings (1–3 hr APF) with a set of sensory organ lineage markers. The sensory organ lineage, the cell-type-specific markers employed, and the rationale behind why these markers were chosen are shown in Figure S3. At 1–3 hr APF in prepupal wings, Sens is expressed at high levels in anterior–dorsal chemosensory SOP as these cells begin their asymmetric divisions. By 8–10 hr APF these divisions are complete, and clusters of differentiated cells corresponding to each dorsal chemosensory bristle are present (Jafar-Nejad *et al.* 2006). Then the mechanosensory SOP cells atop the margin begin to differentiate (Hartenstein and Posakony 1989).

To provide a reference for these results, we examined Sac-lacZ and Dpp-lacZ prepupal wings. Here these genes have the same spatial relationship, to each other and to the SOP markers Sens and Cut, as in larval wings (Ac is not expressed in prepupal wings; Figure S4). One unexpected

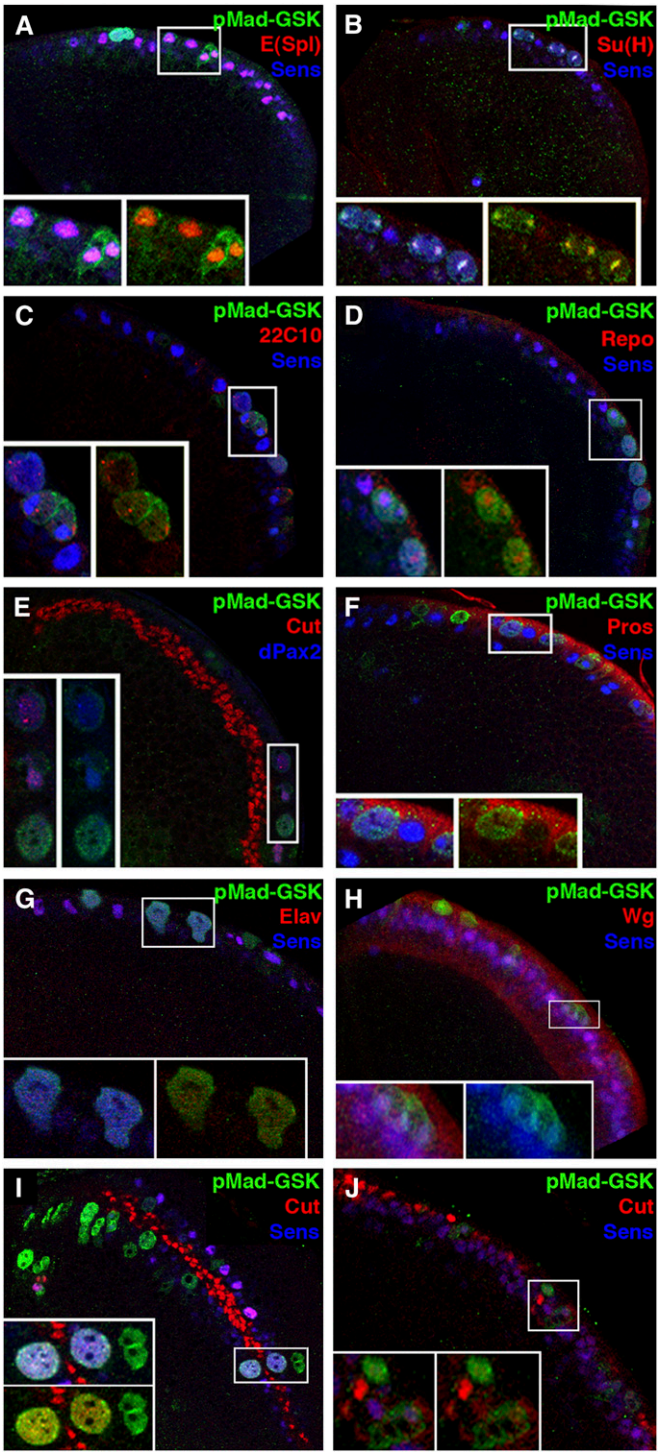

Figure 5 pMad-Gsk is present in sensory organ lineage cells in prepupal wing disks. Single confocal slices of the dorsal side of the anterior margin from a prepupal wing with a Sca-Mad genotype. Except as noted, wings are aged 1–3 hr APF and shown with proximal to the left as in Figure 1A, right inset. Wings display pMad-Gsk (green), Sens (blue), and a cell-type-specific marker (red) except as noted. Overall, pMad-Gsk was present in 11.4 ± 5.6 cells (n = 87), 8.8 ± 4.3 anterior margin cells, 1.1 ± 1.3 L1 sensilla region cells, and 1.6 ± 1.6 L3 sensilla region cells. Boxed areas are enlarged twofold and shown as two insets to better document the subcellular localization of pMad-Gsk: three-color (left) and two-color (pMad-Gsk and marker; right). (A) E(spl)M8 is a transcription factor that marks cells with active Notch signaling (*e.g.*, shaft and neuron). The two E(spl) M8 and Sens cells to the left of the box display uniform pMad-Gsk. (Insets) The E(spl)M8 and Sens endocycling cell on the right with two nuclei displays cytoplasmic pMad-Gsk. (B) Su(H) is a transcription factor that marks the socket cell. (Insets) Three endocycling Su(H) and Sens cells express pMad-Gsk uniformly. (C) Futsch (monoclonal antibody 22C10) is a microtubule-associated protein that marks neurons. (Insets) A 22C10 and Sens endocycling cell on the right with uniformly distributed pMad-Gsk. (D) Repo is a transcription factor marking the transient glial cell. (Insets) The Repo and Sens endocycling cell in the center with two nuclei expresses uniform pMad-Gsk. (E) Cut is a transcription factor and target of Notch that marks the wing margin in a dense row of cells that do not express any sensory organ lineage markers. Cut is also activated in SOP on both sides of the margin by proneural genes and will mark all cells of the sensory organ lineage. dPax2 is a transcription factor that marks SOP, shaft, and sheath cells. (Insets) The three distal-most cells on the ventral surface display varying nuclear concentrations of Cut and dPax2 and also show a transition from cytoplasmic to uniform pMad-Gsk (top to bottom). (F) Pros is a transcription factor normally sequestered in the cytoplasm but that translocates to the nucleus when active in the sheath cell. (Insets) Left cell has nuclear Pros and Sens with uniformly distributed pMad-Gsk while the right cell has cytoplasmic Pros, nuclear Sens, and no pMad-Gsk. (G) Elav is an RNA-binding protein that marks neuronal cells. (Insets) Two endocycling cells express Elav, Sens, and uniform pMad-Gsk. (H) Confocal stack revealing that Wg on the dorsal margin encompasses pMad-Gsk- and Sens-expressing cells. (Insets) Three Sens cells expressing uniform pMad-Gsk. (I) Lateral view of an everting disk at 0–1 hr APF expressing Cut, Sens, and pMad-Gsk. (Insets) The two distal-most Cut and Sens cells that straddle the row of Cut-only margin cells express Cut, Sens, and uniform pMad-Gsk. The cell at the right expresses only uniform pMad-Gsk. The circular empty areas in these cells are likely vesicles as the cell on the left has four of them. (J) At 1–3 hr APF the disk has flattened. (Insets) The Cut and Sens cell on the left displays uniformly distributed pMad-Gsk. The four cells on the right restrict pMad-Gsk to the cytoplasm but only the ventral-most expresses Cut and Sens.

finding was that the SOP lineage on the wing margin is not identical to the lineage of the notum: Sox15, a transcription factor marking the socket cell on the notum (Miller *et al.* 2009), is not present in prepupal wings. As a result, we utilized Su(H) to mark the socket cell. In addition, we found that the transient glial cell (expressing Repo) is present at 1–3 hr APF prior to undergoing apoptosis. An analysis utilizing the apoptosis marker cleaved-Caspase3 confirmed this finding, as no cell death was visible in prepupal wings at 1–3 hr APF.

We found that, in prepupal wings, pMad-Gsk was co-expressed with every one of our cell-type-specific SOP lineage markers (Figure 5). As in larval disks, the number of pMad-Gsk cells was highly variable. Other similarities between pupal and larval pMad-Gsk margin expression were: (1) Wg was always adjacent to pMad-Gsk (Figure 5H), and no disks lacked pMad-Gsk expressing cells; (2) except for dPax2 and Cut (Figure 5, E, I, and J), pMad-Gsk was on the dorsal side; and (3) pMad-Gsk was rarely seen without Sens (Figure 5I).

The subcellular localization of pMad-Gsk varied in pupal wings as it did in larval wings. With all of the markers pMad-Gsk uniform expression (nuclear plus cytoplasm) was the most common (Figure 5). For six of the eight markers, cells with cytoplasmic pMad-Gsk were present as well as cells displaying uniform expression (dPax2: Figure 5E, Cut: Figure 5J). Alternatively, for Repo and Elav cells (Figure 5, D

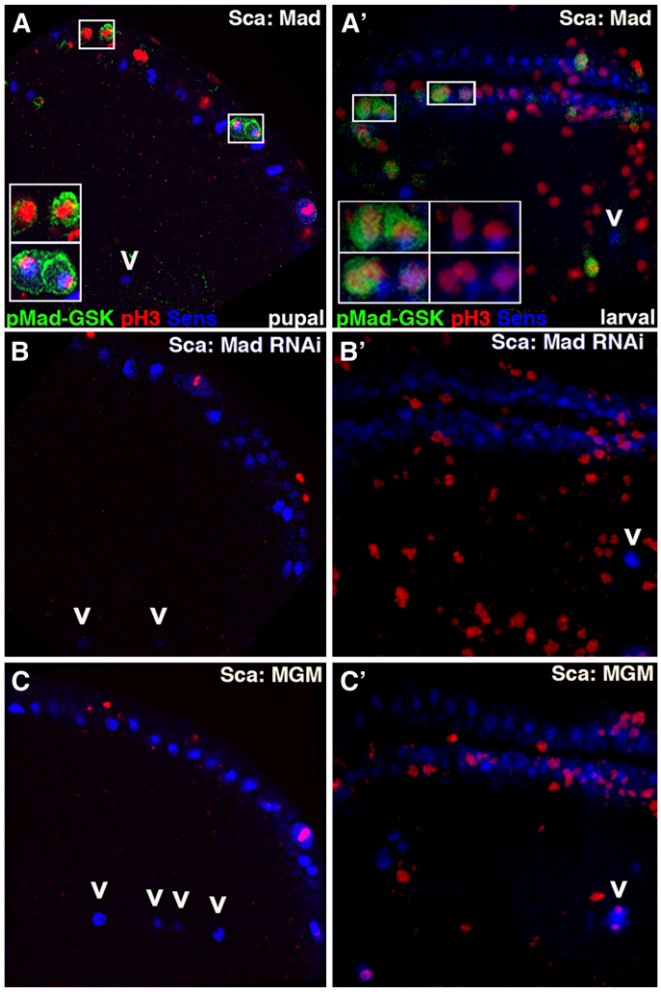

Figure 6 MadRNAi and MGM prepupal wings and larval disks display ectopic Senseless SOP in the anterior–dorsal quadrant. (A–C) Single confocal slices of the anterior–dorsal quadrants of prepupal wings aged and shown as in Figure 3 displaying pMad-Gsk (green), Sens (blue), and the mitotic marker pH3 (red). (A) Sca-Mad wing in which pMad-Gsk is present only in pH3-expressing cells. pH3 cells that do not express pMad-Gsk are also visible. Most but not all pMad-Gsk cells also express Sens. Overall, there were 27.3 ± 12.2 pH3 cells (n = 8), 10.9 ± 5.0 pH3/Sens cells, and 91.5 ± 23.5 Sens cells. Boxed areas are magnified twofold and shown as three-color insets. (Top inset) Two pH3-positive but Sens-negative cells are not visibly dividing and display cytoplasmic pMad-Gsk. (Bottom inset) pH3- and Sens-positive and visibly dividing cell has uniform (cytoplasmic and nuclear) pMad-Gsk. The single Sens cell normally found in the distal L3 sensilla region is shown (arrowhead). (B) Sca-MadRNAi wing lacking pMad-Gsk that overall displays wild-type pH3 and Sens, a phenotype also seen with Sca-Mad, MadRNAi. Overall, there were 36.9 ± 20.3 pH3 cells (n = 15), 18.1 ± 11.7 pH3/Sens cells, and 88.0 ± 47.5 Sens cells. Two Sens cells (one is ectopic) in the distal L3 sensilla region are indicated (arrowheads). (C) Sca-MGM wing lacking pMad-Gsk that overall displays wild-type pH3 and Sens, a phenotype also seen with Sca-Mad, MGM. Overall, there were 37.9 ± 15.7 pH3 cells (n = 8), 14.3 ± 6.6 pH3/Sens cells, and 91.4 ± 34.2 Sens cells. Four Sens cells (three ectopic) in the L3 region are indicated (arrowheads). (A′–C′) Stacked confocal images of the presumptive wing blade in larval disks, aged as shown as in Figure 2. (A′) Sca-Mad disk in which pMad-Gsk is present predominantly on the dorsal surface is found only in pH3-expressing cells and in which only one pMad-Gsk cell does not co-express Sens. Note that not all pH3 cells express pMad-Gsk. A single Sens cell in the distal L3 sensilla region is indicated (arrowhead). Overall, there were 97.6 ± 20.3 pH3 cells (n = 7), 24.0 ± 3.7 pH3/Sens cells, and 146.7 ± 12.3 Sens cells. Boxed areas are enlarged twofold and shown as three-color (left) and two-color (pH3 and Sens, right) insets. (Top and bottom insets) Two pH3- and Sens-positive cells with uniform pMad-Gsk expression. The cell on the left in both is visibly endocycling. (B′) Sca-MadRNAi wing disk lacking pMad-Gsk that displays wild-type pH3 but significantly more Sens cells than Sca-Mad, a phenotype also seen with Sca-Mad, MadRNAi. Overall, there were 121.6 ± 48.1 pH3 cells (n = 11), 25.4 ± 8.46 pH3/Sens cells, and 174.8 ± 43.7 Sens cells. A single Sens cell in the distal L3 sensilla region is indicated (arrowhead). (C′) Sca-MGM wing disk lacking pMad-Gsk that displays wild-type pH3 but a significant excess of Sens cells, a phenotype also seen with Sca-Mad, MGM. Overall, there were 124.0 ± 35.67 pH3 cells (n = 6), 21.2 ± 6.6 pH3/Sens cells, and 244.0 ± 38.3 Sens cells. An inappropriately dividing Sens cell is indicated (arrowhead).

and G), pMad-Gsk was only uniformly expressed. Several experiments suggest that pMad-Gsk is associated with endocycles of DNA replication (without mitosis leading to polyploidy) that occur after the initiation of cell-type-specific gene expression in the neuron, shaft, and socket cells (Hartenstein and Posakony 1989; Audibert *et al.* 2005). For example, E(Spl)M8 (Figure 5A, shaft or neuron), Su(H) (Figure 5B, socket), and 22C10 (Figure 5C, neuron) cells with two nuclei were observed that contain uniform pMad-Gsk. To date, no one has examined endoreplication in the transient glial cell, but cells with two nuclei expressing uniform pMad-Gsk and Repo are visible, suggesting that this cell type also undergoes endocycling (Figure 5D).

Overall, the prepupal wing data support our third hypothesis that Zw3-phosphorylated Mad functions primarily in sensilla and dorsal chemosensory bristle development. Furthermore, the association of pMad-Gsk with non-mitotic endocycles of DNA replication in terminally differentiated sensory organ cells suggests a hypothesis by which MGM (a loss-of-function allele) and Mad-RNAi would lead to ectopic sensory organs. This hypothesis is that the normal function of Zw3-phosphorylated Mad is to restrict mitosis in the sensory organ lineage.

MGM and Mad-RNAi generate ectopic Sens SOP in the anterior–dorsal quadrant of the wing

To test this hypothesis, we analyzed the co-expression of pMad-Gsk, Sens, and the chromosome condensation marker phospho-histone3 (pH3) in prepupal wings expressing Sca-Mad, Sca-MadRNAi, or Sca-MGM. pH3 is generally utilized to mark mitotic cells but is also expressed during endocycles of DNA replication such as those in ovarian follicle cells (Sun *et al.* 2008). If the role of Zw3-phosphorylated Mad in the sensory organ lineage is to restrict mitosis, then MadRNAi and MGM should display more Sens or pH3 cells than the phenotypically wild-type Sca-Mad. We characterized Sca.Gal4 spatial expression in prepupal wings to aid in interpreting these phenotypes. Here the larval relationship between the Sca and Dpp D/V stripes persists: the stripe of Sca overlaps the anterior portion of the parallel stripe of Dpp (Dpp pupal enhancer does not activate until 24 hr APF; Affolter and Basler 2007). As a result, in prepupal wings the Sca

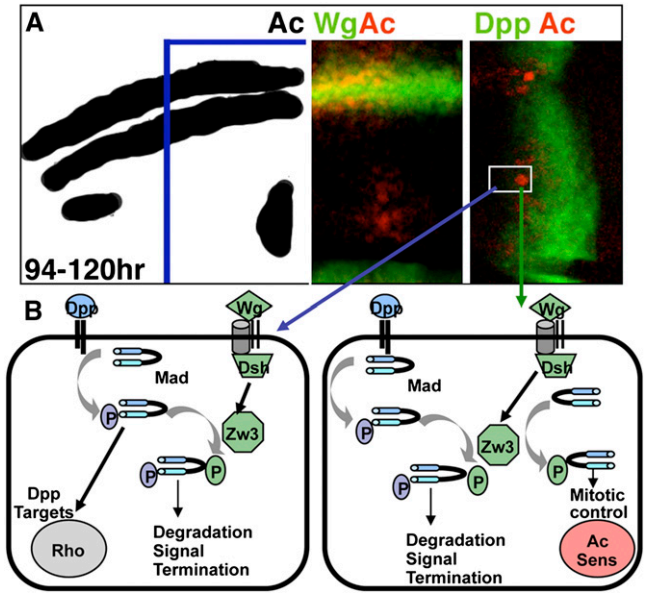

Figure 7 Model of an unconventional Wg pathway leading to Zw3-phosphorylated Mad activity in non-SOP and SOP cells within the anterior–dorsal quadrant of the wing. (A) Schematic of the anterior–dorsal quadrant of a late larval wing disk displaying Ac expression. By this time, Wg activation of Ac has defined the proneural prepattern, and Dpp activation of *spalt* and *omb* has specified vein precursor cells. The outlined section of the margin and L3 sensilla region is shown as two confocal stacks depicting Wg-lacZ and Ac (left) and Dpp-lacZ and Ac (right). Two cells are boxed: a cell expressing high levels of Ac due to feedback from Sens that will become an L3 sensilla SOP (right) and presumably an L3 vein precursor (left) that does not express Ac. (B) Schematic of events occurring within the L3 vein precursor (left) and the L3 SOP sensilla precursor (right). Dpp does not play a primary role in L3 vein specification, but it is nonetheless required upstream of *rhomboid* for proper L3 vein formation (Gomez-Skarmeta and Modolell 1996; Biehs *et al.* 1998). In the L3 vein precursor (left) that does not express Ac or Sens, Wg-dependent Zw3 phosphorylation of Receptor-phosphorylated Mad leads to degradation and the termination of this round of Dpp signaling. Zw3 phosphorylation of nonphosphorylated Mad, if it occurs here, appears to be inconsequential on the basis of the MGM wing phenotype. In the L3 sensilla SOP that expresses Ac and Sens, Wg-dependent Zw3 phosphorylation of nonphosphorylated Mad leads to nuclear accumulation and the restriction of self-renewing mitosis. Zw3 phosphorylation of Receptor-phosphorylated Mad, if it occurs here, may be among the mechanisms used to render these cells nonresponsive to Dpp.

stripe still coincides with the highest levels of Receptor-phosphorylated Mad in the anterior compartment (Figure S4, C and D).

Our examination of pMad-Gsk and pH3 expression in Sca-Mad prepupal wings (which will generally lead to phenotypically normal adult wings; Figure 1A, Table S1A) revealed that pMad-Gsk is present only in pH3-positive cells and that most, but not all, pMad-Gsk cells also express Sens (Figure 6A). As our hypothesis predicts ectopic pH3 and/or Sens expression in the other genotypes, we counted pH3 and Sens cells in Sca-Mad disks and found that expression was highly variable. Sca-MadRNAi prepupal wings lacking pMad-Gsk (25–35% of adult wings have ectopic sensilla or chemosensory bristle duplications; Figure 1B, Table S1B) were not significantly different from Sca-Mad wings. However, we noted that there were ~22% more Sens cells in the L3 sensilla region of Sca-MadRNAi than Sca-Mad (5.8 *vs.* 4.6 Sens cells in the L3 sensilla region). Careful examination revealed that a subset of Sca-MadRNAi wings display a single ectopic Sens cell in this region (Figure 6B). Sca-MGM prepupal wings lacking pMad-Gsk (40–60% of adult wings have ectopic sensilla or chemosensory bristle duplications; Figure 1C, Table S1C) were also not significantly different from Sca-Mad. Again we noted ~25% more Sens cells in the L3 sensilla region (6.0 *vs.* 4.6) because a subset of Sca-MGM wings display one or two ectopic Sens cells in this region (Figure 6C).

The presence of ectopic Sens in the L3 sensilla region of Sca-MadRNAi and Sca-MGM prepupal wings suggested that the defect due to loss of Zw3-phosphorylated Mad occurred in larvae. Examining Sca-Mad larval disks, we noted that pMad-Gsk is present only in pH3-expressing cells and that most, but not all, pMad-Gsk cells also express Sens. At this stage, pH3 cells with uniform (cytoplasmic and nuclear) pMad-Gsk expression are actively dividing (Figure 6A′). In larval disks, pMad-Gsk expression was visible in more cells than in prepupal wings. Sca-MadRNAi larval disks (Figure 6B′) contained similar numbers of pH3 cells and pH3/Sens cells as Sca-Mad but they had significantly more Sens cells (174.8 ± 43.7 *vs.* 146.7 ± 12.3; $P < 0.05$). Sca-MGM larval disks (Figure 6C′) contained similar numbers of pH3 cells and pH3/Sens cells as Sca-Mad, but they also had significantly more Sens cells (244.0 ± 38.3 *vs.* 146.7 ± 12.3; $P < 0.006$). Disks with inappropriately dividing Sens cells in the L3 sensilla region are present even in a small sample of six Sca-MGM disks. The excess of Sens cells in Sca-MadRNAi and Sca-MGM larval disks suggests that the mitotic defect due to loss of Zw3-phosphorylated Mad occurred between the activation of Ac at 95–96 hr AEL and the analysis of Sens at 116–120 hr AEL.

Discussion

Zw3 phosphorylation provokes a distinct response from receptor-phosphorylated and nonphosphorylated Mad

Two studies of Zw3/Gsk3-β phosphorylation of Mad/Smad1 at the homologous sites in flies and vertebrates (Fuentealba *et al.* 2007; Eivers *et al.* 2009) and one of Gsk3-β phosphorylation of Smad3 at a nonhomologous site in mammals (Guo *et al.* 2008) have shown that phosphorylation leads to Smad polyubiquitination, degradation, and TGFβ signal termination. The data predict that blocking this event via site-directed mutagenesis (as in UAS.MGM) would lead to a gain-of-function allele of Mad—one with hyperactivity that generates phenotypes similar to Mad overexpression. Hyperactivity of MGM was reported by those investigators and corroborated by the presence of ectopic veins in our Sca-MGM wing studies. However, detailed analysis of our Sca-MGM wings revealed that hyperactivity is evident only for Mad's Dpp-dependent phenotypes (*e.g.*, ectopic veins). We noted a phenotype in Sca-MGM wings that has not been previously

associated with Dpp signaling: ectopic sensilla and dorsal chemosensory bristle duplications. The sensory organ phenotype was also seen with MadRNAi, suggesting that this subset of the MGM phenotype represents a previously unnoticed loss-of-function phenotype that we have shown is independent of Dpp and Notch and dependent upon Wg signaling.

One simple explanation for the existence of two distinct effects of Zw3 phosphorylation on Mad activity in wing development is that Zw3 phosphorylation influences Receptor-phosphorylated Mad distinctly from nonphosphorylated Mad. We model the unconventional Wg pathway and this biphasic response in Figure 7. If Mad's C-terminal SSVS amino acid sequence is already phosphorylated, then Zw3 phosphorylation in the linker region leads to ubiquitination and signal termination. In the larval wing disk, this occurs in vein precursor cells and results in the ectopic veins of MGM and DN-Zw3 wings as well as the loss of veins in CA-Zw3 and MadRNAi wings. This aspect of the Zw3–Mad interaction is consistent with prior studies and is further supported by Gao *et al.* (2009). On the basis of studies in mammalian cells, they identified Nedd4L and Smurf1 as ubiquitin ligases recognizing doubly phosphorylated (Receptor and Gsk3-β) Smad2/3 or Smad1, respectively. Wnt-induced Zw3 phosphorylation of Receptor-phosphorylated Smads likely represents a conserved mechanism for TGFβ signal termination.

Our Sca.Gal4 wing assays suggested that nonphosphorylated Mad can also respond to Zw3 phosphorylation and that it does so by performing a distinct function. This novel function is the prevention of self-renewing mitotic division by Sens SOP in the anterior–dorsal quadrant of the wing (a region spatially defined by the presence of Apterous and the absence of Engrailed). This novel function of Zw3 phosphorylated but non-Receptor phosphorylated Mad cannot be achieved when MGM and DN-Zw3 are expressed (failure to restrict self-renewing mitosis in Sens SOP leads to ectopic sensory organs) and is hyperactive when CA-Zw3 and Dsh are expressed (complete restriction of Sens SOP mitosis leading to loss of sensilla).

Returning to the studies that prompted this analysis, Eivers *et al.* (2009) reported an increase in Sens expression along the anterior margin in larval disks and overgrowth of dorsal chemosensory bristles in the resulting adult wing when expressing MGM with Scalloped.Gal4. Scalloped.Gal4 is expressed widely on both wing surfaces but maximally at the margin where it is required for formation of bristles (Campbell *et al.* 1992). Eivers *et al.* (2009) concluded that Wg signals through Mad to repress Sens expression in wing development. Our studies agree with the first part of this conclusion and extend their observations by showing that MGM-induced Sens increase is limited to a specific cell type (anterior–dorsal SOP) and is perhaps due to the loss of restriction on self-renewal in those cells. Alternatively, Zeng *et al.* (2008) reported that flip-out clones of Mad repressed Sens and concluded that Receptor-phosphorylated Mad activity antagonizes Wg signaling. In their study, flip-out clones were generated between 72 and 96 hr AEL, before Ac activation by Wg at 94–96 hr AEL and the activation of Sens in SOP. In the earlier period, Dpp and Wg morphogens provide global positional information utilized by cells for their initial cell fate decisions. Thus Dpp antagonism of Wg via Mad during early third instar is likely independent of Wg-stimulated Zw3 phosphorylation of Mad later in wing development.

Recently, an analysis of canonical Wnt signaling in which Gsk3-β moves to the membrane to phosphorylate low density lipoprotein receptor related protein (LRP) co-receptors for signal amplification showed that Gsk3-β is then sequestered into endosomes. This requires β-catenin and effectively isolates Gsk3-β from additional substrates (Taelman *et al.* 2010). Our data showing that Zw3-phosphorylated Mad is associated with an unconventional branch of Wg signaling that does not employ canonical Wg pathway components in their normal way or any canonical components downstream of Zw3 (*e.g.*, dAxin) suggest that Zw3/Gsk3-β sequestration may not be triggered by this mechanism or that sequestration is not rapid or complete enough to prevent Zw3 phosphorylation of Mad.

Zw3-phosphorylated Mad is expressed during mitosis in larval wing disks and functions to prevent Sens SOP self-renewing divisions

The observation that pMad-Gsk is present only in pH3-positive mitotic cells during larval wing development fits with the work of Fuentealba *et al.* (2008) who noted pSmad1-Gsk expression only during self-renewing divisions of human embryonic stem cells. Furthermore, their data revealed that pSmad1-Gsk is asymmetrically segregated into only one of the daughter cells during these divisions. These authors noted that Receptor-phosphorylated Smad1 was also asymmetric (although less so than pSmad1-Gsk). Double phospho-staining experiments were not performed, but our data suggest that the asymmetrically segregated pSmad1 may be the dual phosphorylated form (Receptor and Gsk3-β).

Alternatively, our data show that Zw3-phosphorylated Mad that is not Receptor phosphorylated is present in Sens SOP that are unaffected by TGFβ signaling. These Sens SOP differentiate into two non-identical daughter cells via asymmetric division. As a result, in the presence of Zw3-resistant Mad (MGM), a larval Sens SOP undergoes a single self-renewing division prior to its typical differentiation division to generate an ectopic Sens SOP that becomes either an ectopic sensilla or an ectopic dorsal chemosensory bristle. Thus, the activity of Zw3-phosphorylated Mad may be influenced by several factors: the presence of Receptor phosphorylation, the cell type, and the type of mitosis (self-renewal *vs.* differentiation).

The nuclear accumulation of pMad-Gsk during mitosis in larval Sens SOP shares several features with the behavior of Zw3 observed with a GFP-exon trap allele in third instar larval central brain neuroblasts (Wojcik 2008). During differentiation (*i.e.*, an asymmetric division generating a new neuroblast and a distinct ganglion mother cell) it was shown that Zw3 is cytoplasmic during interphase and prophase. At the onset of metaphase, Zw3 nuclear accumulation begins and is

visible through cytokinesis when Zw3 becomes cytoplasmic again in each of the two new cells. These similarities suggest that perhaps Zw3-phosphorylated Mad and/or Zw3 may contribute to a common function in these cells: facilitation of differentiating *vs.* self-renewing division in cells capable of both.

New features of Wg, Sens, and Mad activity in wing development

Our data also illuminate new aspects of wing and sensory organ formation. From a global patterning perspective, we provide new insights into how Hedgehog (Hh) and its signal transducer Cubitus interruptus (Ci) influence L3 sensilla development. Mullor *et al.* (1997) showed that ectopic Hh throughout the anterior compartment led to numerous ectopic L3 veins that were accompanied by sensilla. In their view, these cells were fooled into thinking that they were L3 cells close to normal Hh at the A/P compartment boundary. Subsequently, Methot and Basler (2001) showed that *Ci* loss-of-function clones in the posterior compartment can generate an ectopic sensilla on L4. Here the interpretation was that Hh activation of Engrailed is lost in clones, and thus a cell was fooled into thinking that it was in the anterior compartment near Hh at the A/P compartment boundary. Alternatively, no reports suggest Hh has any role in the differentiation of SOP into sensilla. Mullor *et al.* (1997) explicitly invoke an independent factor X between Hh and L3 sensilla differentiation. Our data suggest that the most logical candidate is Wg.

Thus, we propose that Wg continues to influence wing disk development late in the third instar, beyond its roles in global D/V patterning early in the third instar and Ac activation in mid-third instar. With regard to the biochemical underpinnings of the unconventional pathway leading to Zw3 phosphorylation of Mad during late third instar development, we note that the mechanism underlying canonical Wg pathway interactions between Frizzled and Dsh and between Dsh and Zw3 is also currently unknown. It is tempting to speculate that an interaction between Zw3 and Dark-dependent caspase (Kanuka *et al.* 2005) that does not involve cell death but instead influences the formation of mechanosensory bristles on the notum may play a role.

We extend the identification of Sens as the primary factor in chemosensory bristle specification to the specification of sensilla in the anterior–dorsal quadrant. The basis for this extension may be that all cells in the anterior–dorsal quadrant express Apterous and none express Engrailed. Thus Sens plays the same role in all SOP within this genetically and spatially defined quadrant. Alternatively, the stout mechanosensory bristles on the margin for which Sens serves as a proneural gene, independent of Ac and Scute, derive from the anterior–ventral quadrant that does not express Apterous or Engrailed. Distinct consequences associated with Sens function in SOP development in the two quadrants may necessitate the restriction of self-renewing mitosis by Zw3-phosphorylated Mad to the anterior–dorsal quadrant.

Intriguingly, our data identify the first known non-TGFβ-dependent role for any Smad protein in any organism. While many non-Smad-signaling pathways are activated by TGFβ receptors, to date Smads have not been reported to have any functions independent of TGFβ signaling. Even the initial studies of Zw3-phosphorylated Mad indicated that this event served to terminate TGFβ signaling. We are examining the possibility that Mad has additional TGFβ-independent roles by analyzing the effect of EGFR/MapK signaling on Mad phosphorylation.

In summary, during wing development the phosphorylation of Mad by Zw3 is not a mechanism of pathway crosstalk but instead represents a spatially localized round of unconventional Wg signaling during sensory organ development. This signal limits the self-renewal of Sens SOP cells, and this limitation may be necessary for SOP cells to differentiate via asymmetric division leading to adult sensory organs. The conservation of Zw3 phosphorylation sites in Mad's vertebrate homologs suggests that this mechanism may be widely utilized for balancing self-renewal and differentiation during development.

Acknowledgments

We are especially grateful to Eddy DeRobertis for sharing reagents prior to publication. We thank the Bloomington Stock Center, Hugo Bellen, Sarah Bray, the Developmental Studies Hybridoma Bank, Ed Eivers, Ken Irvine, Ed Laufer, Mike O'Connor, Jim Posakony, John Reinitz, and Francois Schweisguth for flies, antibodies, and valuable discussions. The authors declare no competing financial interests.

Literature Cited

Affolter, M., and K. Basler, 2007 The Dpp morphogen gradient: from pattern formation to growth regulation. Nat. Rev. Genet. 9: 663–674.

Aldaz, S., L. M. Escudero, and M. Freeman, 2010 Live imaging of *Drosophila* imaginal disc development. Proc. Natl. Acad. Sci. USA 107: 14217–14222.

Andrews, H., N. Giagtzoglou, S. Yamamoto, K. Schulze, and H. Bellen, 2009 Sequoia regulates cell fate decisions in the sensory organs of *Drosophila*. EMBO Rep. 6: 636–641.

Audibert, A., F. Simon, and M. Gho, 2005 Cell cycle diversity involves differential regulation of cyclin E activity in the *Drosophila* bristle cell lineage. Development 132: 2287–2297.

Axelrod, J., K. Matsuno, S. Artavanis-Tsakonas, and N. Perrimon, 1996 Interaction between Wingless and Notch signaling mediated by *dishevelled*. Science 271: 1826–1832.

Bangi, E., and K. Wharton, 2006 Dual function of the Drosophila Alk1/Alk2 ortholog *Sax* shapes the BMP activity gradient in the wing. Development 133: 3295–3303.

Biehs, B., M. Sturtevant, and E. Bier, 1998 Boundaries in the *Drosophila* wing imaginal disc organize vein-specific genetic programs. Development 125: 4245–4257.

Blackman, R., M. Sanicola, L. Raftery, T. Gillevet, and W. Gelbart, 1991 An extensive 3′ cis-regulatory region directs the imaginal disk expression of *dpp*, a member of the TGFβ family in *Drosophila*. Development 111: 657–665.

Blair, S., 1992 shaggy (zeste-white 3) and the formation of supernumerary bristle precursors in the developing wing blade of *Drosophila*. Dev. Biol. 152: 263–278.

Blair, S., A. Giangrande, J. Skeath, and J. Palka, 1992 Development of normal and ectopic sensilla in *hairy* and *Hairy wing* mutants of *Drosophila*. Mech. Dev. 38: 3–16.

Bourouis, M., 2002 Targeted increase in *shaggy* activity levels blocks Wingless signaling. Genesis 34: 99–102.

Brand, A., and N. Perrimon, 1993 Targeted gene expression as a means of altering cell fates and generating dominant phenotypes. Development 118: 401–415.

Brand, M., A. Jarman, L. Jan, and Y. Jan, 1993 *asense* is a Drosophila neural precursor gene and is capable of initiating sense organ formation. Development 119: 1–17.

Brummel, T., S. Abdollah, T. Haerry, M. Shimell, J. Merriam *et al.*, 1999 The Activin receptor Baboon signals through dSmad2 and controls cell proliferation but not patterning during larval development. Genes Dev. 13: 98–111.

Campbell, S., M. Inamdar, V. Rodrigues, V. Raghavan, M. Palazzolo *et al.*, 1992 The *scalloped* gene encodes a novel, evolutionarily conserved transcription factor required for sensory organ differentiation in *Drosophila*. Genes Dev. 6: 367–379.

Carroll, S., and J. Whyte, 1989 The role of the *hairy* gene during *Drosophila* morphogenesis: stripes in imaginal disks. Genes Dev. 3: 905–916.

Chen, Y., M. Riese, M. Killinger, and F. Hoffmann, 1998 A genetic screen for modifiers of *Drosophila dpp* signaling identifies *punt*, *Mad* and *60A*. Development 125: 1759–1768.

Couso, J., S. Bishop, and A. Martinez Arias, 1994 The *wingless* signaling pathway and the patterning of the wing margin in *Drosophila*. Development 120: 621–636.

Couso, J., E. Knust, and A. Martinez Arias, 1995 *Serrate* and *wingless* cooperate to induce *vestigial* gene expression and wing formation in *Drosophila*. Curr. Biol. 5: 1437–1448.

Cubas, P., J. de Celis, S. Campuzano, and J. Modolell, 1991 Proneural clusters of *acheate-scute* expression and the generation of sensory organs in the *Drosophila* wing disc. Genes Dev. 5: 996–1008.

de Celis, J., and S. Bray, 1997 Feed-back mechanisms affecting Notch activation at the dorsoventral boundary in the *Drosophila* wing. Development 124: 3241–3251.

de Celis, J., J. de Celis, P. Ligoxygakis, A. Preiss, C. Delidakis *et al.*, 1996 Functional relationships between *Notch*, *Su(H)* and the bHLH genes of the *E(spl)* complex: the *E(spl)* genes mediate only a subset of Notch activities during imaginal development. Development 122: 2719–2728.

Derynck, R., and K. Miyazono, 2008 *The TGFβ Family* Cold Spring Harbor Laboratory Press, Cold Spring Harbor, NY.

Dworkin, I., and G. Gibson, 2006 EGFR and TGF-β signaling contributes to variation for wing shape in Drosophila. Genetics 173: 1417–1431.

Eivers, E., L. Fuentealba, V. Sander, J. Clemens, L. Hartnett *et al.*, 2009 *Mad* is required for *wg* signaling in wing development and segment patterning in *Drosophila*. PLoS ONE 4: e6543.

Fortini, M., I. Rebay, L. Caron, and S. Artavanis-Tsakonas, 1993 An activated Notch receptor blocks cell-fate in the developing *Drosophila* eye. Nature 365: 555–557.

Fuentealba, L., E. Eivers, A. Ikeda, C. Hurtado, H. Kuroda *et al.*, 2007 Integrating patterning signals: Wnt/GSK3 regulates the duration of the BMP/Smad1 signal. Cell 131: 980–993.

Fuentealba, L., E. Eivers, D. Geissert, V. Taelman, and E. DeRobertis, 2008 Asymmetric mitosis: unequal segregation of proteins destined for degradation. Proc. Natl. Acad. Sci. USA 105: 7732–7737.

Funakoshi, Y., M. Minami, and T. Tabata, 2001 *mtv* shapes the activity gradient of the Dpp morphogen through regulation of *thickveins*. Development 128: 67–74.

Gao, S., C. Alarcon, G. Sapkota, S. Rahman, P. Chen *et al.*, 2009 Ubiquitin ligase Nedd4L targets activated Smad2/3 to limit TGFβ signaling. Mol. Cell 36: 457–468.

Gho, M., M. Lecourtois, G. Geraud, J. W. Posakony, and F. Schweisguth, 1996 Subcellular localization of S(H) in *Drosophila* sense organ cells during Notch signaling. Development 122: 1673–1682.

Gomez-Skarmeta, J., and J. Modolell, 1996 *araucan* and *caupolican* provide a link between compartment subdivisions and patterning of sensory organs and veins in the *Drosophila* wing. Genes Dev. 10: 2935–2945.

Guo, M., L. Jan, and Y. Jan, 1996 Control of daughter cell fates during asymmetric division: interaction of Numb and Notch. Neuron 17: 27–41.

Guo, X., A. Ramirez, D. Waddell, Z. Li, X. Liu *et al.*, 2008 Axin and GSK3-β controls Smad3 protein stability and modulate TGFβ signaling. Genes Dev. 22: 106–120.

Haerry, T., O. Khalsa, M. O'Connor, and K. Wharton, 1998 Synergistic signaling by two BMP ligands through the Sax and Tkv receptors controls wing growth and patterning in *Drosophila*. Development 125: 3977–3987.

Hartenstein, V., and J. Posakony, 1989 Development of adult sensilla on the wing and notum of *Drosophila*. Development 107: 389–405.

Hays, R., G. Gibori, and A. Bejsovec, 1997 W signaling generates pattern through two distinct mechanisms. Development 124: 3727–3736.

Hayward, P., T. Kalmar, and A. Arias, 2008 Wnt/Notch signaling and information processing during development. Development 135: 411–424.

Hoodless, P., T. Haerry, S. Abdollah, M. Stapleton, M. O'Connor *et al.*, 1996 MadR1, a Mad-related protein in BMP2 signaling. Cell 85: 489–500.

Jafar-Nejad, H., M. Acar, R. Nolo, H. Lacin, H. Pan *et al.*, 2003 Senseless acts as a binary switch during sensory organ precursor selection. Genes Dev. 17: 2966–2978.

Jafar-Nejad, H., A. Tien, M. Acar, and H. Bellen, 2006 Senseless and Daughterless confer neuronal identity to epithelial cells in the wing. Development 133: 1683–1692.

Jarman, A., and I. Ahmed, 1998 The specificity of proneural genes in determining *Drosophila* sense organ identity. Mech. Dev. 76: 117–125.

Jennings, B., A. Preiss, C. Delidakis, and S. Bray, 1994 The Notch pathway is required for E(spl) expression during neurogenesis in *Drosophila*. Development 120: 3537–3548.

Kanuka, H., E. Kuranaga, K. Takemoto, T. Hiratou, H. Okano *et al.*, 2005 *Drosophila* caspase transduces Shaggy/GSK-3β kinase activity in neural precursor development. EMBO J. 21: 3793–3806.

Kassis, J., E. Noll, E. VanSickle, W. Odenwald, and N. Perrimon, 1992 Altering the insertional specificity *Drosophila* transposable elements. Proc. Natl. Acad. Sci. USA 89: 1919–1923.

Khalsa, O., J. Yoon, S. Torres-Schumann, and K. Wharton, 1998 TGFβ/BMP superfamily members, Gbb-60A and Dpp, cooperate to provide pattern information and establish cell identity in the *Drosophila* wing. Development 125: 2723–2734.

Kosman, D., S. Small, and J. Reinitz, 1998 Rapid preparation of a panel of polyclonal antibodies to *Drosophila* segmentation proteins. Dev. Genes Evol. 208: 290–294.

Lai, E., F. Roegiers, X. Qin, Y. Jan, and G. Rubin, 2005 The ubiquitin ligase Mind bomb promotes Notch signaling by regulating the localization and activity of Serrate and Delta. Development 132: 2319–2332.

Logan, C., and R. Nusse, 2004 The Wnt signaling pathway in development and disease. Annu. Rev. Cell Dev. Biol. 20: 781–810.

Marquez, R., M. Singer, N. Takaesu, W. Waldrip, Y. Kraytsberg *et al.*, 2001 Transgenic analysis of the Smad family of TGFβ signal transducers in Drosophila suggests new roles and new interactions. Genetics 157: 1639–1648.

Masucci, J., R. Miltenberger, and F. Hoffmann, 1990 Pattern-specific expression of the *Drosophila dpp* gene in imaginal disks is regulated by 3′ cis-regulatory elements. Genes Dev. 4: 2011–2023.

Methot, N., and K. Basler, 2001 An absolute requirement for Ci in Hh signaling. Development 128: 733–742.

Milan, M., F. Diaz-Benjumea, and S. Cohen, 1998 *Beadex* encodes an LMO protein that regulates Apterous LIM-homeodomain activity in *Drosophila* wing development: a model for LMO oncogenes function. Genes Dev. 12: 2912–2920.

Miller, S., T. Avidor-Reiss, A. Polyanovsky, and J. Posakony, 2009 Complex interplay of three transcription factors in controlling the tormogen differentiation program of *Drosophila* mechanoreceptors. Dev. Biol. 329: 386–399.

Moore, A., F. Roegiers, L. Jan, and Y. Jan, 2004 Conversion of neurons and glia to external-cell fates in the sensory organs of *Drosophila hamlet* mutants by a cousin-cousin cell-type re-specification. Genes Dev. 18: 623–628.

Mullor, J., M. Calleja, J. Capdevila, and I. Guerero, 1997 Hedgehog activity, independent of *dpp*, participates in wing disc patterning. Development 124: 1227–1237.

Nakao, K., and J. A. Campos-Ortega, 1996 Persistent expression of genes of the *E(spl)* complex suppresses neural development in *Drosophila*. Neuron 162: 275–286.

Newfeld, S., and R. Wisotzkey, 2006 Molecular evolution of Smad proteins, pp. 15–35 in *Smad Signal Transduction*, edited by C.-H. Heldin and P. ten Dijke. Springer-Verlag, Berlin; Heidelberg, Germany; New York.

Newfeld, S., E. Chartoff, J. Graff, D. Melton, and W. Gelbart, 1996 *Mad* encodes a conserved cytoplasmic protein required in Dpp/TGFβ responsive cells. Development 122: 2099–2108.

Nishita, M., M. Hashimoto, S. Ogata, M. Laurent, N. Ueno *et al.*, 2000 Interaction between Wnt and TGFβ signaling pathways during formation of Spemann's organizer. Nature 403: 781–785.

Nolo, R., L. A. Abbott, and H. Bellen, 2000 Senseless a Zn finger transcription factor is necessary and sufficient for sensory organ development *Drosophila*. Cell 102: 349–362.

Papayannopoulos, V., A. Tomlinson, V. Panin, C. Rauskolb, and K. Irvine, 1998 D/V signaling in the *Drosophila* eye. Science 281: 2031–2034.

Penton, A., Y. Chen, K. Staehling-Hampton, J. Wrana, L. Attisano *et al.*, 1994 Identification of two BMP Type I receptors in Drosophila and evidence that Brk25D is a *dpp* receptor. Cell 78: 239–250.

Persson, U., H. Izumi, S. Souchelnytskyi, S. Itoh, S. Grimsby *et al.*, 1998 The L45 loop in type I receptors for TGFβ family members is a critical determinant in specifying Smad isoform activation. FEBS Lett. 434: 83–87.

Powell, P., C. Wesley, S. Spencer, and R. Cagan, 2001 Scabrous complexes with Notch to mediate boundary formation. Nature 409: 626–630.

Quijano, J., M. Stinchfield, B. Zerlanko, Y. Gibbens, N. Takaesu *et al.*, 2010 The *Sno* oncogene antagonizes Wingless signaling in wing disks of *Drosophila*. PLoS ONE 5: e11619.

Raftery, L., V. Twombly, K. Wharton, and W. Gelbart, 1995 Genetic screens to identify elements of the *dpp* pathway in Drosophila. Genetics 139: 241–254.

Ray, R., and K. Wharton, 2001 Context-dependent relationship between the BMPs *gbb* and *dpp* during development of the *Drosophila* wing disk. Development 128: 3913–3925.

Rebay, I., R. Fehon, and S. Artavanis-Tsakonas, 1993 Specific truncations of *Drosophila* Notch define activated and dominant negative forms of the receptor. Cell 74: 319–329.

Sander, V., E. Eivers, R. Choi, and E. M. DeRobertis, 2010 *Drosophila* Smad2 opposes *Mad* signaling during wing vein development. PLoS ONE 5: e10383.

Sekelsky, J., S. Newfeld, L. Raftery, E. Chartoff, and W. Gelbart, 1995 Genetic characterization and cloning of *Mad*, a gene required for *dpp* function in Drosophila. Genetics 139: 1347–1358.

Siegfried, E., T. Chou, and N. Perrimon, 1992 *wg* signaling acts through *zw3*, the *Drosophila* homolog of *gsk-3*, to regulate *en* and establish cell fate. Cell 71: 1167–1179.

St. Johnston, D., F. Hoffmann, R. Blackman, D. Segal, R. Grimaila *et al.*, 1990 Molecular organization of the *dpp* gene in *Drosophila*. Genes Dev. 4: 1114–1127.

Staehling-Hampton, K., and F. Hoffmann, 1994 Ectopic *dpp* in the *Drosophila* midgut alters the expression of homeotic genes, *dpp* and *wg*, causing specific morphological defects. Dev. Biol. 164: 502–512.

Sun, J., L. Smith, A. Armento, and W. Deng, 2008 Regulation of the endocycle/gene amplification switch by Notch and ecdysone signaling. J. Cell Biol. 182: 885–896.

Taelman, V., R. Dobrowolski, J. Plouhinec, L. Fuentealba, P. Vorwald *et al.*, 2010 Wnt signaling requires sequestration of Gsk3 inside multivesicular endosomes. Cell 143: 1136–1148.

Takaesu, N., E. Herbig, D. Zhitomersky, M. O'Connor, and S. Newfeld, 2005 DNA-binding mutations in Smad genes yield dominant-negative proteins or a neomorphic protein that can activate Wg target genes in *Drosophila*. Development 132: 4883–4894.

Tweedie, S., M. Ashburner, K. Falls, P. Leyland, P. McQuilton *et al.*, 2009 FlyBase: enhancing *Drosophila* gene ontology annotations. Nucleic Acids Res. 37: D555–D559.

Twombly, V., E. Bangi, V. Le, B. Malnic, M. Singer *et al.*, 2009 Functional analysis of *sax*, the Drosophila gene encoding the BMP type I receptor ortholog of human Alk1 and Alk2. Genetics 183: 563–579.

Van Doren, M., P. Powell, D. Pasternak, A. Singson, and J. Posakony, 1992 Spatial regulation of proneural gene activity: auto- and cross-activation of *acheate* is antagonized by *emc*. Genes Dev. 6: 2592–2605.

Willert, K., C. Logan, A. Arora, M. Fish, and R. Nusse, 1999 A *Drosophila* Axin homolog, dAxin, inhibits Wnt signaling. Development 126: 4165–4173.

Wisotzkey, R., A. Mehra, D. Sutherland, L. Dobens, X. Liu *et al.*, 1998 *Medea* is a *Drosophila Smad4* homolog that is differentially required to potentiate Dpp responses. Development 125: 1433–1445.

Wisotzkey, R., A. Johnson, N. Takaesu, and S. Newfeld, 2003 α/β Hydrolase2, a predicated gene adjacent to *Mad* in *Drosophila*, belongs to a new global multigene family and is associated with obesity. J. Mol. Evol. 56: 351–361.

Wojcik, E., 2008 A mitotic role for GSK-3β kinase in *Drosophila*. Cell Cycle 7: 3699–3708.

Zeng, C., S. Younger-Shepherd, L. Jan, and Y. Jan, 1998 Delta and Serrate are redundant Notch ligands required for asymmetric cell divisions within the *Drosophila* sensory organ lineage. Genes Dev. 12: 1086–1091.

Zeng, Y., M. Rahnama, S. Wang, W. Lee, and E. Verheyen, 2008 Inhibition of *Drosophila* Wg signaling involves competition between Mad and Arm for dTcf. PLoS ONE 3: e3893.

Zheng, X., J. Wang, T. Haerry, A. Wu, J. Martin *et al.*, 2003 TGF-β signaling activates steroid hormone receptor expression during neuronal remodeling in the *Drosophila* brain. Cell 112: 303–315.

Communicating editor: J. A. Birchler

GENETICS

Supporting Information
http://www.genetics.org/content/suppl/2011/08/25/genetics.111.133801.DC1

Wg Signaling via Zw3 and Mad Restricts Self-Renewal of Sensory Organ Precursor Cells in *Drosophila*

Janine C. Quijano, Michael J. Stinchfield, and Stuart J. Newfeld

DOI: 10.1534/genetics.111.133801

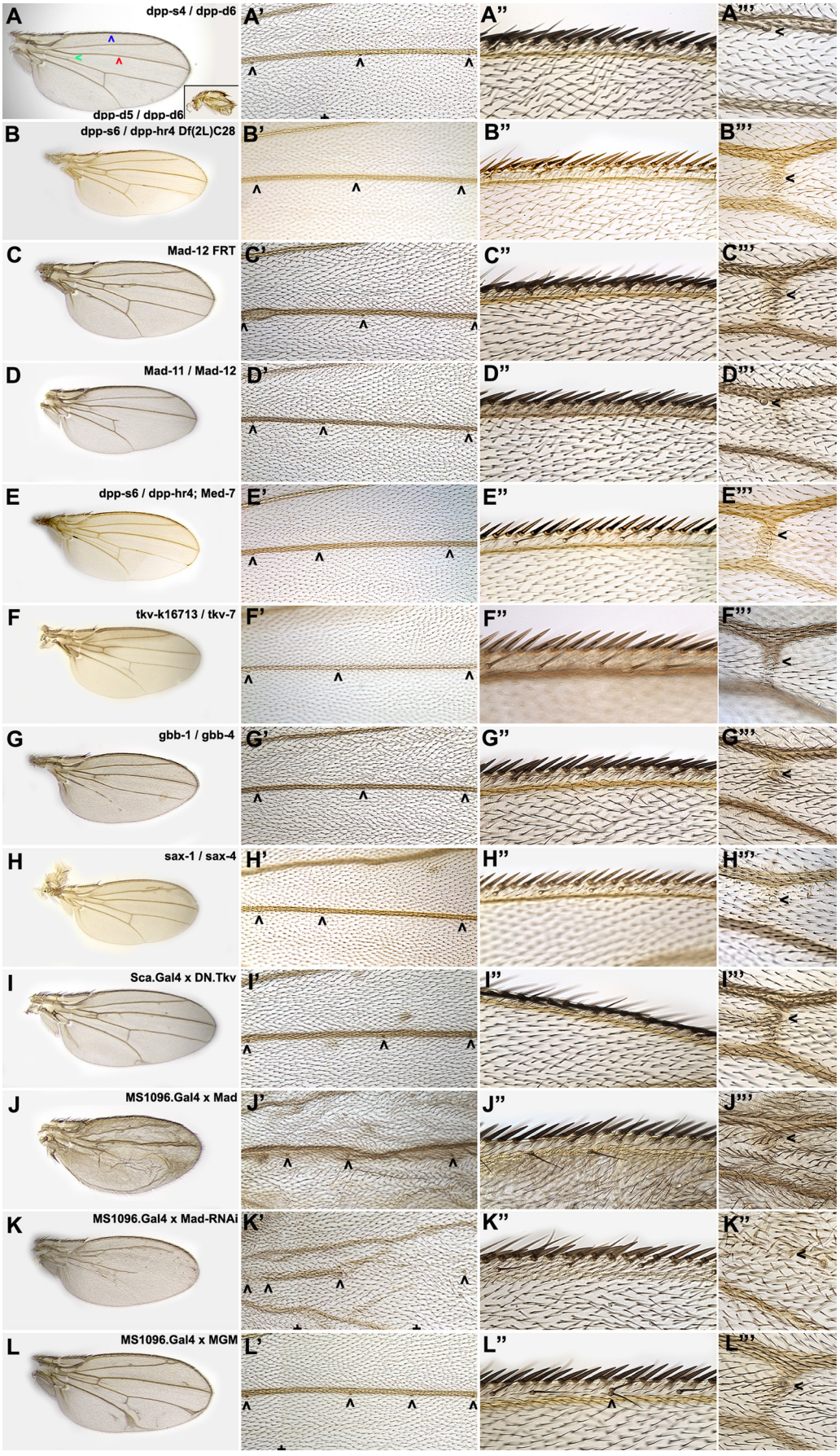
A
dpp-s4 / dpp-d6
dpp-d5 / dpp-d6
A'
A"
A"'
B
dpp-s6 / dpp-hr4 Df(2L)C28
B'
B"
B"'
C
Mad-12 FRT
C'
C"
C"'
D
Mad-11 / Mad-12
D'
D"
D"'
E
dpp-s6 / dpp-hr4; Med-7
E'
E"
E"'
F
tkv-k16713 / tkv-7
F'
F"
F"'
G
gbb-1 / gbb-4
G'
G"
G"'
H
sax-1 / sax-4
H'
H"
H"'
I
Sca.Gal4 x DN.Tkv
I'
I"
I"'
J
MS1096.Gal4 x Mad
J'
J"
J"'
K
MS1096.Gal4 x Mad-RNAi
K'
K"
K"'
L
MS1096.Gal4 x MGM
L'
L"
L"'

Figure S1 No ectopic sensory organs are present in Dpp/Gbb/Activin pathway genotypes except MadRNAi and MGM. Whole wing image with high magnification views of the L3 sensilla, dorsal margin bristles and ACV sensilla. A) dpp^{s4} / dpp^{d6} wing missing the anterior crossvein (ACV; green arrowhead) but with normal L3 sensilla (red arrowhead) and dorsal chemosensory bristles (blue arrowhead). The sensillum that is normally located on the dorsal surface of the ACV is present in its usual P/D location but has relocated to the dorsal surface of L3 since the ACV is missing. Inset - dpp^{d5} / dpp^{d6} wing shown to scale that has a discernable costa on the proximal anterior margin and an alula on the proximal posterior margin but no wing blade. B) dpp^{s6} / dpp^{hr4} *Df(2L)C28* wing with longitudinal and crossvein truncations and normal L3/ACV sensilla and dorsal chemosensory bristles. C) Wing with unmarked clones of the non-Receptor phosphorylatable allele Mad^{12}. Numerous vein loops are visible where loss of *Mad* disrupts vein formation but the L3/ACV sensilla and dorsal chemosensory bristles are normal. D) Mad^{12} / Mad^{11} wing with longitudinal, ACV and posterior crossvein (PCV) truncations but with normal L3 sensilla and dorsal chemosensory bristles. The ACV sensillum is again relocated to the dorsal surface of L3 since the ACV is missing. E) dpp^{s6} / dpp^{hr4} Med^{7} wing with longitudinal and crossvein truncations but normal L3/ACV sensilla and dorsal chemosensory bristles. F) $P\{lacW\}tkv^{k16713}$ / tkv^{7} wing with PCV truncation but normal L3/ACV sensilla and dorsal chemosensory bristles. G) gbb^{1}/ gbb^{4} wing with longitudinal truncations and missing crossveins but normal L3 and dorsal chemosensory bristles. The ACV sensillum is present even though the ACV is truncated. H) sax^{1} / sax^{4} wing with truncated ACV and ectopic vein tissue near L2 but normal L3 sensilla and dorsal chemosensory bristles. The ACV sensillum is present even though the ACV is truncated. I) Sca-DN-Tkv wing with longitudinal and crossvein truncations plus ectopic vein tissue associated with L2, L3 and the ACV. The L3/ACV sensilla and dorsal chemosensory bristles are normal. J) MS1096-Mad wing with an oversized L3 vein along its entire length but truncations of L4, L5 and the crossveins. The L3 sensilla are normal, the dorsal chemosensory bristles are disorganized but otherwise normal and the ACV sensillum is present without an ACV. K) MS1096-MadRNAi wing missing most of the longitudinal and crossveins. An ectopic sensillum is present in the L3 region proximal to the normal L3 sensilla and the distal-most L3 sensilla is present without any L3 vein. The dorsal chemosensory bristles are normal and the ACV sensillum is present in the correct location without any ACV or L3 present. L) MS1096-MGM wing with ectopic tissue associated with all longitudinal veins and a truncation of the PCV. An ectopic sensillum is present on L3 and dorsal chemosensory bristles duplications are visible. The ACV sensillum is normal.

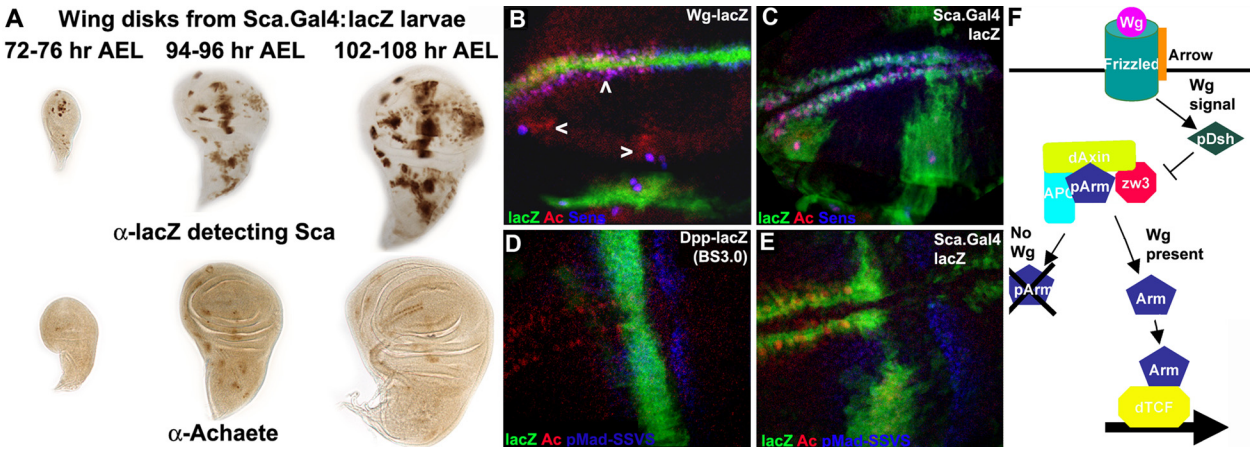

Figure S2 Temporal and spatial relationship of Sca, Ac and Sens to Wg and Dpp in larval wing disks. A) Temporal relationship of Sca (top row) and Ac (bottom row) expression is shown utilizing wing disks from staged third instar larvae with anterior to the left as in Fig. 1A left inset. Sca is visible in patches of the wing blade in the youngest larva with expression expanding with larval age. Ac expression is first seen in scattered individual cells on the notum and the L1 and L3 sensilla regions 20 hours later and in two rows along the anterior margin roughly six hours after that. B-E) Spatial relationships are shown in stacked confocal images of the presumptive wing blade with anterior to the left displaying lacZ (green), Ac (red) and Sens or pMad-SSVS (blue). B) Wg-lacZ disk with expression in a stripe running A/P emanating from the D/V boundary that also encircles the presumptive wing blade and will become the entire wing margin (the upper and lower domains of Wg are connected outside the field of view). Ac and Sens are visible bracketing the upper Wg stripe in one dorsal row (below Wg) and one ventral row (above Wg) of margin bristle SOP (middle arrowhead). Ac is expressed in the anterior compartment only (left side) while Wg and Sens are expressed in both compartments. Ac and Sens expressing SOP in the proximal region of L1 (left arrowhead) and the distal region of L3 (right arrowhead) are also visible. C) Sca-lacZ disk with Sca expression in every Ac and Sens cell on the margin and in a wide domain that encompasses the Ac and Sens cells in the L1 sensilla region. Sca is also present in a broad D/V stripe in the center of the disk that encompasses the Ac and Sens cells of the L3 region and coincides with the posterior-most (distal-most in the adult wing) Ac expressing margin cells. D) Dpp-lacZ disk driven by the BS3.0 reporter gene displaying a D/V stripe of expression that lies just anterior to the A/P compartment boundary (BLACKMAN *et al.* 1991). pMad-SSVS expression is visible in two concentration gradients (decreasing toward the anterior and toward the posterior). Both gradients begin adjacent to the A/P compartment boundary where no pMad-SSVS is present due to the activity of the *tkv* repressor *scribbler* (FUNAKOSHI *et al.* 2001). Dpp expression overlaps the origin of the anterior pMad-SSVS gradient, encompasses the posterior-most Ac expressing cells on the margin and the Ac cells in the L3 region. E) Sca-lacZ disk with pMad-SSVS expression again visible in two gradients. Sca-lacZ overlaps the origin of the anterior gradient and encompasses the posterior-most margin and L3 region Ac cells. The D/V stripe of Sca-lacZ considerably overlaps the parallel stripe of Dpp expression. F) Schematic of the canonical Wg pathway. Wg signal transduction begins with the Frizzled2 Receptor and the Arrow Co-Receptor. The receptor complex activates Dsh via an unknown mechanism. Dsh then relays the signal to a ubiquitous cytoplasmic complex of Zw3, dAPC, dAxin and Arm. Under non-signaling conditions, Zw3 phosphorylation continuously shunts the ubiquitously expressed Arm into the proteasome pathway for degradation. Upon a Wg signal Dsh prevents Zw3 prevented from phosphorylating Arm again via an unknown mechanism. This leads to Arm nuclear accumulation and activation of gene expression in cooperation with dTCF.

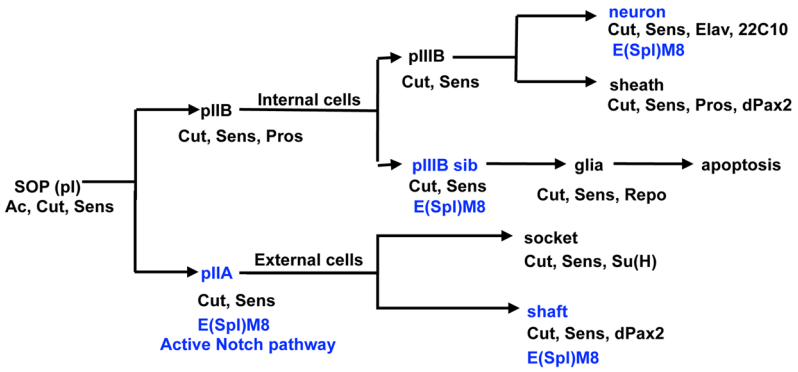

Figure S3 The wing sensory organ lineage, Notch activity and cell type specific markers employed in this study. The current model for the lineage leading from a single larval SOP cell (pI) to the four cells of a mechanosensory bristle on the adult notum is shown (MILLER *et al.* 2009). Horizontal lines indicate daughters and vertical lines indicate siblings. Markers for each cell type utilized in Fig. 5 are shown below each cell. Asymmetric cell divisions resulting in Notch activity and expression of the Notch pathway effector E(spl)M8 in one of the daughter cells are shown in blue. An initial asymmetric division of pI yields a pIIA and a pIIB cell. The pIIA cell gives rise to the external shaft and socket cells after another asymmetric division. The pIIB cell gives rise to the internal cells and divides asymmetrically to form pIIIB and pIIIBsib cells. The pIIIB cell divides asymmetrically to generate the sheath and extrasensory neuron. The pIIIBsib differentiates into a glial cell that eventually undergoes apoptosis.

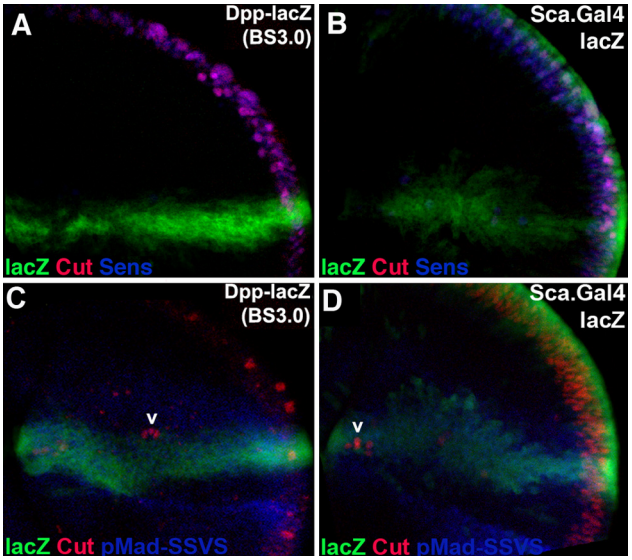

Figure S4 Spatial relationship of Sca, Cut and Sens to Wg and Dpp in pre-pupal wings. Stacked confocal images of pre-pupal wings aged and shown as in Fig. 3 displaying lacZ (green), Cut (red) and Sens or pMad-SSVS (blue). A) Dpp-lacZ disk shows that the larval D/V stripe of Dpp expression that lies just anterior to the A/P compartment boundary persists into the pre-pupal stage as a stripe along the P/D axis. The Dpp stripe maintains is relationship to the perpendicular rows of Cut and Sens expression along the margin. B) Sca-lacZ disk shows that the larval D/V stripe of Sca expression persists into the pre-pupal stage as a stripe along the P/D axis. The Sca stripe is still wider than the Dpp stripe as it extends into the anterior compartment. Sca is present along the anterior margin in concert with Cut and Sens expression. C) Dpp-lacZ disk shows that pMad-SSVS near the margin maintains its larval expression as two gradients - diminishing toward the anterior and posterior with the same relationship to Dpp expression. Near the region of the L3 sensilla (shown by Cut expression; arrowhead), the separation between the pMad-SSVS gradients disappears and single bidirectional gradient coincident with Dpp expression extends proximally. D) Sca-lacZ disk shows that Sca maintains the same relationship to Dpp and pMad-SSVS expression as in larval disks (L3 region Cut expression; arrowhead).

Table S1 Wing phenotypes of Sca.Gal4 x Mad, MadRNAi and MGM or zw3-M11 clones

A. Sca.Gal4 x Mad

Total Wings	phenotype	#/phenotype	%/phenotype[a]
522	wild type	179	34.3%
	ectopic vein tissue posterior to L5	146	28.0%
	ectopic vein tissue L3	86	16.5%
	ectopic vein tissue L5	58	11.1%
	ectopic vein tissue PCV	23	4.4%

B. Sca.Gal4 x MadRNAi

Total Wings	phenotype	#/phenotype	%/phenotype
370	wild type	0	0.0%
	small wing	370	100.0%
	L5 truncates at PCV	370	100.0%
	L3 truncates where ACV should be	370	100.0%
	ACV missing	370	100.0%
	gap in L4	356	96.2%
	dorsal chemosensory bristle duplications	96	26.0%
	PCV truncates before L5	66	17.8%
	4-5 sensilla on L3 (dorsal)	53	14.3%
	3 or more sensilla on L1 (dorsal)	52	14.2%
	stout mechanosensory bristle transformed to chemosensory	14	3.8%
	ectopic thin mechanosensory bristle L1 (dorsal)	19	3.6%

C. Sca.Gal4 x MGM

Total wings	phenotype	#/phenotype	%/phenotype
500	wild type	173	34.6%
	3 or more sensilla on L1 (dorsal)	201	40.2%
	dorsal chemosensory bristle duplications	183	36.6%
	4-5 sensilla on L3 (dorsal)	177	35.3%
	ectopic vein tissue posterior to L5	119	23.8%
	ectopic vein tissue L5	96	19.2%
	ectopic vein tissue L2	60	12.0%
	ectopic vein tissue L3	22	4.4%
	ectopic thin mechanosensory bristle L1 (dorsal)	22	4.4%

D. FRT-101 zw3-M11

Total Wings	phenotype	#/phenotype	%/phenotype
30	wild type	0	0.0%
	4-5 sensilla on L3 (dorsal)	30	100.0%
	margin bristle duplications (all types)	30	100.0%
	numerous tufts of ectopic bristles (all types)	27	90.0%
	gap in L4	5	16.7%
	PCV truncates before L5	4	13.3%
	ectopic vein tissue L2	4	13.3%
	ectopic vein tissue L5	2	6.7%

a - A percentage for each phenotype is shown to indicate relative frequency:

1) Percentages may not sum to 100% as those occurring less than 3% are excluded except wild type

2) Percentage sum may exceed 100% because an individual wing can display multiple phenotypes

Table S2 Wing Phenotypes for Dpp/Gbb/Activin Pathway Mutants[a]

A. dpp-d6/dpp-d5

Total Wings	phenotype	#/phenotype	%/phenotype[b]
58	wild type	0	0.0%
	very small wing with no blade (all veins and sensilla gone)	58	100.0%
	dorsal/ventral surfaces unattached throughout	58	100.0%
	ectopic thin mechanosensory bristle on wing blade[c]	4	6.9%

B. dpp-s6/dpp-hr4

Total wings	phenotype	# phenotype	% phenotype
736	wild type	620	84.2%
	gap in L4	59	8.0%
	L2 truncates before margin	44	6.0%

C. dpp-s4/dpp-d6

Total wings	phenotype	#/phenotype	%/phenotype
28	wild type	0	0.0%
	ACV missing	26	93.0%
	ectopic thin mechanosensory bristle L3 (ventral)[c]	2	7.2%

D. Mad-12 FRT-40A

Total wings	phenotype	#/phenotype	%/phenotype
404	wild type	164	40.6%
	vein loop L2	131	32.4%
	gap or vein loop L3	88	21.8%
	vein loop L5	28	6.9%
	gap in PCV	14	3.5%

E. Mad-12/Mad-11

Total wings	phenotype	#/phenotype	%/phenotype
17	wild type	0	0.0%
	small wing	17	100.0%
	L4 truncated	17	100.0%
	ACV missing	8	47.1%

F. FRT-82B Med-8

Total wings	phenotype	#/phenotype	%/phenotype
514	wild type	192	37.4%
	ectopic vein tissue PCV	150	29.2%
	vein loop L3	100	19.5%
	L3 bifurcates at the margin	63	12.3%
	L2 and L1 prematurely merged at the margin	55	10.7%
	vein loop L2	53	10.3%
	L4 bifurcates at the margin	28	5.4%
	PCV truncated	19	3.7%

G. dpp-s6/dpp-hr4 Df(2L)C28

Total wings	phenotype	#/phenotype	%/phenotype
14	wild type	0	0.0%
	truncated L4	12	85.7%
	truncated L2	7	50.0%
	PCV missing	1	7.1%

H. dpp-s6/dpp-hr4; Med

Total wings	phenotype	# Phenotype	% Phenotype
6	wild type	0	0.0%
	truncated L4	5	83.3%
	small undeveloped wing	1	16.7%

I. tkv-k16713 /tkv-7

Total Wings	phenotype	#/phenotype	%/phenotype
15	wild type	1	6.6%
	ectopic vein tissue PCV	11	73.0%
	ACV truncated	6	40.0%
	ectopic stout mechanosensory bristle dorsal margin[c]	2	13.0%
	PCV truncated	1	6.6%
	ectopic vein tissue L3	1	6.6%

J. Sca.Gal4 x DN-Tkv

Total wings	phenotype	#/phenotype	%/phenotype
36	wild type	15	41.7%
	ACV truncated	10	27.8%
	PCV truncated	8	22.2%
	ACV missing	4	11.1%

K. gbb-1/gbb-4

Total Wings	phenotype	#/phenotype	%/phenotype
32	wild type	0	0.0%
	PCV missing	32	100.0%
	L5 truncated	32	100.0%
	ACV truncated	31	96.9%
	L4 truncated	21	65.6%
	L1 and L2 merge prematurely at the margin	11	34.4%
	excessive spacing between dorsal chemosensory bristles[c]	10	31.2%

L. sax-1/sax-4

Total Wings	phenotype	#/phenotype	%/phenotype
80	wild type	42	52.5%
	L1 and L2 merge prematurely at the margin	31	38.8%
	ACV missing	13	16.3%

M. FRT-18A dSmad2-mb388

Total Wings	phenotype	#/phenotype	%/phenotype
398	wild type	369	97.6%

N. Sca.Gal4 x CA-Tkv

Total wings	phenotype	#/phenotype	%/phenotype
260	wild type	4	1.5%
	dorsal chemosensory bristles too close together[c]	161	61.9%
	ectopic vein tissue L3	154	59.2%
	ectopic vein tissue L5	144	55.4%
	ectopic stout mechanosensory bristle on dorsal margin[c]	17	6.5%
	ectopic vein tissue L2	17	6.5%

O. Sca.Gal4 x CA-Sax

Total Wings	phenotype	#/phenotype	%/phenotype
380	wild type	25	6.6%
	ectopic vein tissue L2	305	80.2%
	ectopic vein tissue PCV	97	25.5%
	ectopic vein tissue L5	55	14.5%
	dorsal chemosensory bristles too close together[c]	41	10.8%

P. Sca.Gal4 x Gbb

Total Wings	phenotype	#/phenotype	%/phenotype
410	wild type	337	82.2%
	dorsal chemosensory bristles too close together[c]	66	16.1%

Q. MS1096.Gal4 x Mad

Total Wings	phenotype	#/phenotype	%/phenotype
472	wild type	0	0.0%
	dorsal/ventral surfaces unattached L5 region	472	100.0%
	L4 and L5 veins truncated	472	100.0%
	ACV and PCV missing	472	100.0%
	excessive spacing between dorsal chemosensory bristles[c]	216	45.8%

R. MS1096.Gal4 x MadRNAi

Total Wings	phenotype	#/phenotype	%/phenotype
524	wild type	0	0.0%
	all veins truncated	524	100.0%
	ACV and PCV missing	524	100.0%
	ectopic stout mechanosensory bristle dorsal margin[c]	25	4.8%

S. MS1096.Gal4 x MGM

Total Wings	phenotype	#/phenotype	%/phenotype
418	wild type	0	0.0%
	dorsal/ventral surfaces unattached L2 and L3 distal region	418	100.0%
	4-5 sensilla on L3 (dorsal)	366	87.5%
	3 or more sensilla on L1 (dorsal)	243	58.3%
	dorsal chemosensory bristle duplications	140	33.3%
	no distinction between costa and anterior wing margin	126	30.1%
	ectopic vein tissue L3	84	20.1%
	ectopic thin mechanosensory bristle L3 (ventral)[c]	70	16.6%
	L4 bifurcates at margin	51	12.2%
	ectopic tissue L2	43	10.3%
	L2 bifurcates at margin	24	5.7%

a - Mutants analyzed: 1) *dpp; dpp^{d5} / dpp^{d6}* (hypomorph affecting larval functions) and *dpp^{s6} / dpp^{hr4}* (hypomorph affecting pupal functions) and *dpp^{s4} / dpp^{d6}* (hypomorph affecting larval/pupal functions; ST. JOHNSTON *et al.* 1990), 2) *Mad; Mad^{12}* clones and the *Mad^{12} / Mad^{11}* hypomorph (*Mad^{11}* is an allele with 25% of the strength of *Mad^{12}* in quantitative tests; TAKAESU *et al.*

2005), 3) *Medea; Med*^{8} clones (*Med*^{8} is a genetic null for Dpp signaling; WISOTZKEY *et al.* 1998), 4) *dpp Mad* and *dpp Med* combinations with enhanced *dpp* pupal wing phenotypes; *dpp*^{s6} / *dpp*^{hr4} *Df(2L)C28* and *dpp*^{s6} / *dpp*^{hr4} *Med*^{7} (TAKAESU *et al.* 2005), 5) *tkv; P{lacW}tkv*^{k16713} / *tkv*^{7} (hypomorph; DWORKIN and GIBSON 2006) and Sca-DN-Tkv (HAERRY *et al.* 1998). 6) *gbb*; *gbb*^{1}/ *gbb*^{4} (hypomorph; RAY and WHARTON 2001), 7) *sax*; *sax*^{1} / *sax*^{4} - (hypomorph; TWOMBLY *et al.* 2009) and 8) *dSmad2; dSmad2*^{MB388} clones (a genetic null; ZHENG *et al.* 2003).

b - Percentages are shown as in Table S1.

c - In a few genotypes we observed a low frequency of anterior margin bristle disorganization (e.g. inappropriate distance between chemosensory bristles or mild intermingling of the chemosensory and stout mechanosensory bristle rows). As these margin phenotypes appeared in genotypes with prominent vein defects, we attribute them to irregularities in the underlying L1 vein due to the reduction/loss of Dpp/Gbb signaling and not to defects in sensory organ formation. Supporting evidence is derived from chemosensory bristle counts in genotypes with disorganized margins. Wild type females have 18.0 $\pm$ 8.4 (n=64) and males 16.9 $\pm$ 8.1 bristles (n=72). *gbb*^{1} / *gbb*^{4} flies with vein defects in and what appear to be gaps in the chemosensory bristle row actually have wild type counts (females 19.3 $\pm$ 6.4, n=87; males 17.4 $\pm$ 7.7, n=70). Thus, modest disorganization of margin bristle rows does not automatically suggest defective sensory organ formation. In addition, we identified occasional freestanding ectopic bristles (as opposed to duplications) and bristle transformations (e.g., stout to thin mechanosensory). This suggests previously unappreciated genetic variability in bristle formation similar to that reported for wing shape (DWORKIN and GIBSON 2006).

T**able S3 Wing phenotypes of Sca.Gal4 x CA-Zw3, Dsh, DN-Zw3 and dAxinDRGS**

A. Sca.Gal4 x Mad, CA-Zw3

Total wings	phenotype	#/phenotype	%/phenotype[a]
53	wild type	0	0.0%
	no sensilla on L1	53	100.0%
	no sensilla on L3	53	100.0%
	all types of margin bristles missing	53	100.0%
	L1 vein truncated	53	100.0%
	costal vein truncated	36	75.5%
	ectopic bristle L3 distal	12	22.6%
	L4 truncated	6	11.3%
	L5 truncated	4	7.6%

B. Sca.Gal4 x Mad, Dsh

Total wings	phenotype	#/phenotype	%/phenotype
39	wild type	0	0.0%
	0-1 sensilla on L1	39	100.0%
	0-2 sensilla on L3	39	100.0%
	L3 thick	39	100.0%
	ectopic bristles L3 (dorsal)	39	100.0%
	ectopic mechanosensory bristles dorsal margin	39	100.0%
	ACV truncated	15	38.5%
	vein loop L3	14	35.9%
	ectopic vein tissue L1	11	28.2%
	ACV missing	10	25.6%
	ectopic vein tissue L2	6	15.4%
	ectopic vein tissue L5	5	12.8%

C. Sca.Gal4 x Mad, DN-Zw3

Total wings	phenotype	#/phenotype	%/phenotype
104	wild type	37	35.5%
	ectopic vein tissue L5	67	64.4%
	ectopic vein tissue L3	39	37.5%
	L5 trifurcates at margin	32	30.8%
	L3 thick	31	29.8%
	ACV truncated	10	9.6%
	ectopic mechanosensory bristles dorsal margin	9	8.6%
	4-5 sensilla on L3 (dorsal)	7	6.6%
	L5 thick	6	5.8%
	vein loop L5	5	4.8%
	vein loop L3	5	4.8%

D. Sca.Gal4 x Mad, dAxinDRGS

Total wings	phenotype	#/phenotype	%/phenotype
24	wild type	0	0.0%
	all types of margin bristles missing	24	100.0%
	ectopic vein tissue L3	9	37.5%
	ectopic vein tissue L5	6	25.0%

a - Percentages are shown as in Table S1.